TAMPERE UNIVERSITY OF TECHNOLOGY

Mahwish Zahra

Linearity of Outphasing Radio Transmitters

Master of Science Thesis

Examiners: Prof. Mikko Valkama,
Dr. Lauri Anttila
Examiner and topic approved by the
Faculty of Computing and Electrical Engineering
on May 5^{th}, 2014

ABSTRACT

TAMPERE UNIVERSITY OF TECHNOLOGY
Master's Degree Programme in Electrical Engineering
Zahra, Mahwish Linearity of Outphasing Radio Transmitters
Master of Science Thesis, 50 pages, 2 Appendix pages
June 2016
Major: Wireless Communications Circuits and Systems
Examiners: Prof. Mikko Valkama, Dr. Lauri Anttila
Keywords: ACLR, Imbalances, Linearity, Outphasing Transmitter

The outphasing transmitter is a promising technique, which can simultaneously achieve high linearity and power efficiency, thereby addressing the major design requirements of next generation transmitters. It employs highly non-linear power amplifier (PA) classes in a linear manner, in principle transmitting a distortion-free signal. Due to symmetric nature of the outphasing architecture, its linearity performance is constrained by any mismatches and non-linear effects encountered in the RF paths. This thesis analyzes the linearity performance of outphasing transmitters (in terms of ACLR specification) for LTE base station applications, under the non-linear effects and tolerances present in practical implementations.

The system-level model, built in Matlab software, investigates the important non-linear effects present in outphasing transmitters, including gain and phase imbalance, IQ modulator mismatches, delay imbalance, and the non-linear effects of PAs and Chireix combiners. The path and delay mismatches result in only partial cancellation of the wideband quadrature signal, and thus create interference in both the in-band and out-of-band frequency regions. The misalignment in IQ modulators, such as gain/phase imbalance and carrier leakage, introduces amplitude and phase modulation in the outphased signals. The quadrature modulator mismatches, in conjunction with amplifier nonlinearity, result in spectral regrowth around the carrier frequency. The transmitter linearity performance is also affected by mismatches in the non-linear characteristics of the PAs. Realistic square-wave signals, exhibiting finite rise- and fall- time, also create spectral leakage for distinct rise/fall times in each outphasing branch. Furthermore, the Chireix combiner severely degrades the linearity of outphasing transmitters; it produces ACLR well below the specified limit for LTE base stations. This makes mandatory the compensation of Chireix combiner induced non-linearity in outphasing transmitters.

The strict linearity requirements (for LTE downlink applications) present a small tolerance window for mismatches experienced in practical circuits. The relatively small tolerance margin indicates the need of linearization and compensation techniques in outphasing transmitters.

ACKNOWLEDGMENTS

I start with the Name of Allah, the most Beneficent and Merciful

Many people have contributed to the successful completion of my master's thesis. First, I would like to express my gratitude to my supervisors, Prof. Mikko Valkama and Dr. Lauri Anttila, for introducing me to the subject of outphasing transmitters. Their guidance, understanding and patience added considerably to my research experience. Overall, it was a great learning opportunity, which gave me a chance to explore new subjects and test my abilities.

I would also like to thank Jaakko Marttila and Markus Allen for their helpful writing tips on using Latex. Additionally, I am grateful to Enrico Roverato, Jerry Lemberg, Prof. Jussi Ryynänen, Kari Stadius, Marko Kosunen, Mikko Martelius, and Tero Nieminen from Aalto University for their numerous technical discussions on the performance of outphasing transmitters. I am greatly indebted to my colleague members of AATU-project for making a supportive environment as a team, and their contributions to the project.

Finally, I am grateful to my parents for having faith in me, and providing me with unparalleled support throughout my thesis. I would also like to thank my siblings, Ali and Sanae, for always being there to lift my spirits.

May 24^{th}, 2016
MAHWISH ZAHRA

CONTENTS

LIST OF ACRONYMS

3GPP	3rd Generation Partnership Project
ACLR	Adjacent Channel Leakage Ratio
AM	Amplitude Modulation
AM-AM	Amplitude to Amplitude Conversion
AM-PM	Amplitude to Phase Conversion
BER	Bit Error Rate
CMCD	Current-Mode Class D PA
DAC	Digital-to-Analog converter
FET	Field Effect Transistor
FOH	First-Order Hold
GSM	Global System for Mobile Communications
IQ	In-phase and Quadrature
LINC	Linear Amplification using Non-linear Components
LPA	Linear Power Amplifier
LO	Local Oscillator
LTE	Long Term Evolution
MLINC	Multi-level Linear Amplification using Non-linear Components
MQAM	M-ary Quadrature Amplitude Modulation
OFDM	Orthogonal Frequency-Division Multiplexing
OOB	Out-of-Band
OT	Outphasing Transmitter
PAPR	Peak-to-Average Power Ratio
PM	Phase Modulated
PAE	Power Added Efficiency

PA	Power Amplifier
PDF	Probability Density Function
RF	Radio Frequency
SCS	Signal Component Seperator
SMPA	Switch-Mode Power Amplifier
TDMA	Time Division Multiple Access
TL	Transmission-Line
VMCD	Voltage-Mode Class D PA
ZOH	Zero-Order Hold

LIST OF SYMBOLS

a	Linear gain of non-linear PA
$\alpha(t)$	Amplitude modulation of the input signal
α_{max}	Maximum amplitude level of input signal envelope
α_o	Half of α_{max}
c	Third-order characteristics of non-linear PA
$e(t)$	Quadrature signal
η	Instantaneous efficiency
G	Intrinsic gain of Linear PA
γ	Electrical stub length
Γ	Reflection coefficient
$\phi(t)$	Phase modulation of the input signal
$\theta(t)$	Outphasing angle
$S_{RF,k}$	RF phase modulated signals
$S_{OUT}(t)$	Combiner output signal at RF
$s_{out}(t)$	Complex envelope of combiner output signal
τ	Delay mismatch
$x(t)$	Input signal
y	Normalized characteristic admittance of Chireix combiner

List of Figures

1. INTRODUCTION

Wireless communications has become an essential part of 21^{st} century lifestyle. We are always in-touch with our family, friends and colleagues with cell phones and aware of the happenings around the world through social media. The advent of mobile internet has increased the demand for broadband access. This rise in usage of wireless data communications comes with the ever-increasing need for more bandwidth, a limited and non-renewable resource. Likewise, the operational costs of mobile radio networks is increasing, as base stations and data centers are consuming more power due to increased processing. On the other hand, climate change emphasizes the need for radio networks to shift to green technologies. These factors present energy consumption as a critical design factor for next generation transceivers.

The power budget of a transceiver is consumed chiefly by RF power amplifier, the component amplifying low level signal to high power for transmission over a wireless channel. In 1990s, 2G mobile communication technologies (GSM = Global System for Mobile Communications , TDMA = Time Division Multiple Access) were designed, transmitting low data rates while employing constant envelope modulation schemes. However these schemes couldn't cope with the increasing demand for higher data rates. As can be seen in Figure 1.1, the spectral occupancy of constant envelope modulated signal is inefficient compared to a variable envelope signal with complex modulation, given that the two signals have the same data rate. Targeting to achieve higher data rates, 3G and 4G systems utilized complex modulation schemes (OFDM = Orthogonal Frequency-Division Multiplexing, MQAM = M-ary

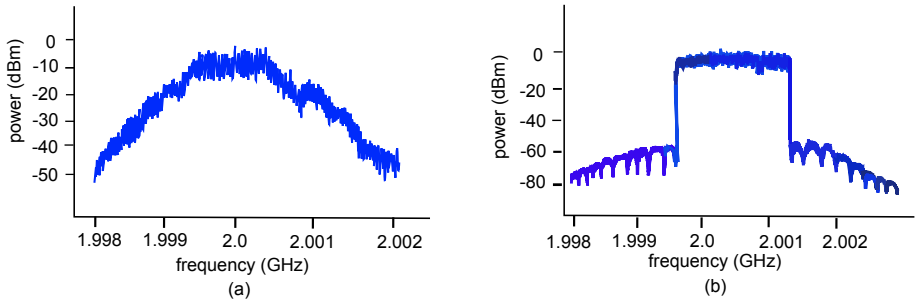

Figure 1.1: Signal power spectrum: (a) constant envelope signal, (b) variable envelope signal with complex modulation [1].

Quadrature Amplitude Modulation) - exploiting both amplitude and phase modulation to transfer data. The spectral efficiency achieved from complex modulation format results in increased signal dynamics; placing stringent requirements on PA efficiency and linearity [2].

In the past, RF PAs were trans-conductance based amplifiers, where the transistors (FET = Field Effect Transistor) act as current sources being controlled by the signal at its gate. The bias point of those active devices determines the conduction angle (varying between zero and 2π for different classes) – the main defining factor for efficiency and linearity of linear amplifiers. If these amplifiers are operated in linear mode, they provide low efficiency and vice versa.

The need for efficient transmission led to the switched-mode PA (class D, E and F), where the transistors are biased to act as switches. In on-state, they are driven to operate in the region of small resistance during conduction, ideally short circuit. Conversely they have no current flow during off-state, thus acting as an open circuit. The overall power consumption of the active devices reduces significantly, ideally being equal to zero.

Power amplifiers trade-off between power efficiency and linearity. Efficient PAs operate in non-linear mode which introduces distortion [3]. Consequently, the amplifier is operated at low signal levels (large back-off) to meet certain bit error rate (BER) and linearity requirements in transmitters. Unfortunately, spectrally efficient modulation formats like OFDM exhibit high Peak-to-Average Power Ratio (PAPR), thus requiring a large back-off, and leading to a significantly reduced efficiency. Consequently, a single-ended PA structure cannot exhibit high linearity and power efficiency concurrently [2].

Moreover, the advancement in circuit fabrication, primarily in lithography techniques, along with the shrinking voltage headroom and design of fast transistors with improved matching, has increased the timing resolution of integrated circuits, favoring techniques that employ pure phase modulation [4].

Outphasing is one such technique which applies phase modulation to achieve linear and efficient amplification of high PAPR signals. Also known as Linear Amplification using Non-linear Components (LINC), it converts amplitude and phase modulated input signal into two pure phase modulated signals. These two signals are decomposed in such a manner that their summation produces the original signal. The outphased signals can be amplified using highly non-linear power amplifiers, while obtaining a linearly amplified signal after combining operation [5],[6]. Thus, the outphasing transmitter takes advantage of the advancement in integrated circuit technology and power amplification techniques, with huge potential for next generation transceivers.

2. OUTPHASING TRANSMITTER

Mobile applications in smart phones require high data transfer speeds. 3G and 4G systems utilize complex block modulation formats to support high data rate connections. These modulation schemes exploit both amplitude and phase modulation to transmit data in a spectral efficient manner. However, this increases the signal dynamics, thus raising minimum linearity requirements for PAs.

A key indicator for signal envelope variation is the peak-to-average power ratio (PAPR). As the name suggests it is the ratio of instantaneous peak power maxima and average transmitted power, formally defined as [7],[8]

$$PAPR = 10log_{10}\frac{max|x(t)|^2}{E(|x(t)|^2)}.$$

Orthogonal Frequency Division Multiplexing (OFDM) is a widely utilized modulation technique for high data rate wireless applications. It consists of a large number of parallel narrow-band sub-carriers, each sub-carrier carries a portion of the transmitted data. As a result OFDM signals are robust against narrow-band interference and multi-path fading effects. However, they exhibit high dynamic range or PAPR and any non-linearity encountered in the transmitter chain can heavily distort OFDM signal and corrupt information bits. Unfortunately, linear amplifiers do not offer energy efficient operation, whereas efficient amplifiers are generally highly non-linear. The outphasing transmitter architecture moderates this trade-off between efficiency and linearity in power amplifiers by transforming a varying envelope signal into two constant envelope signals, which are amplified using two independent non-linear PAs and combined before transmission. The following sections discuss the power amplifier classes, the outphasing transmitter concept and its performance.

2.1 RF Power Amplifiers

The power amplifier is a critical element in determining linearity and efficiency of transmitters. It amplifies a low level signal to higher power, ensuring adequate received power in a wireless channel. Naturally, it dominates the power budget of the transmitters, whether mounted in base-stations or cell phone transceivers. PAs increase the cost of base station operations due to their excessive energy consump-

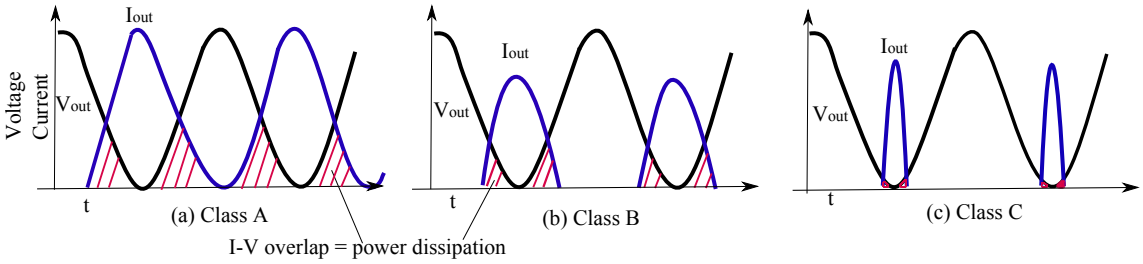

Figure 2.1: Characteristic output waveforms for linear power amplifiers.

tion. Most of this energy is wasted as heat, requiring additional cooling equipment and further increasing the power consumption. Likewise, it reduces battery life of mobile phones - a much needed resource in the age of smart phones with many power hungry mobile applications and added functionality.

Conventional linear power amplifiers operate the transistor, of final amplifying stage, as a current source with relatively high average output impedance. Class-A, B, AB, C comprise the linear class of power amplifiers [9]. Figure 2.1 shows the output voltage and current waveforms for Class-A, B and C amplifiers. These amplifiers utilize non-linear (saturation and pinch-off) regions of transistors (FET) to achieve optimal efficiency. But operating power amplifiers in the non-linear region introduces a great amount of distortion especially for high PAPR signals. Consequently, linear PAs are constrained to operate at low power levels, known as back-off mode, to preserve signal integrity. Efficiency of the linear amplifiers reduces with delivered load power, measured as power added efficiency (PAE) [3], defined as

$$PAE = \frac{P_{OUT} - P_{IN}}{P_{DC}}.$$

Here, P_{OUT}, P_{IN} are the output and input RF power respectively and P_{DC} is the supplied DC power.

Transistors in conducting-class amplifiers operate in transconductance mode, it yields high current and voltage levels simultaneously, resulting in higher power dissipation. Linear PAs employ the transistor as a current source, it's average output impedance is relatively high. They offer high linearity and low power efficiency.

Power consumed by an amplifier can be reduced by minimizing overlap of transistor output voltage and current waveforms. The transistor does not have direct control over its drain voltage waveform (V_{out}) in transconductance mode. But if the transistor operates as a switch, toggling between on-state and off-state, PA designers can easily control the voltage waveform [10]. Thus, to attain higher efficiency, one or more active devices need to be operated as a switch, introducing the concept of switch-mode power amplifiers (SMPA).

SMPAs drive transistors to operate as on-off switches. When the switch is closed,

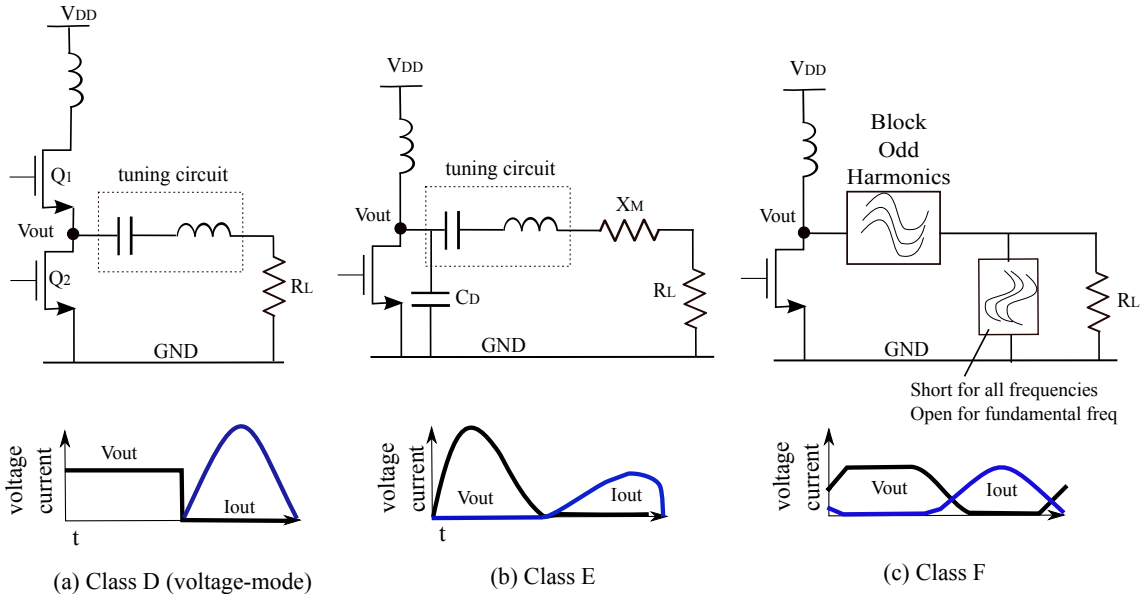

(a) Class D (voltage-mode) (b) Class E (c) Class F

Figure 2.2: Schematics and output current/voltage waveforms of switch-mode PA.

AC current flows into it, and when it is open, AC current flows through the load generating output voltage. Ideally, SMPAs have non-overlapping square shaped voltage and current waveforms (across the transistor), resulting in 100% power efficiency for lossless switches. Class D, E and F PAs are classified as switch-mode power amplifiers.

Class-D amplifiers are realized with a pair of active devices and a tuning circuit. The transistor pair operates in push-pull mode, one transistor conducts constant current in the time period the other one is switched off. The waveform at pair's output node (V_{out}) is square-wave, resonator converts the output current into a sinusoidal waveform. It is passed through a resistor to obtain sinusoidal output voltage. Class D power amplifier ideally converts all DC power to fundamental frequency power. Class D amplifiers are further grouped into Voltage-mode Class D (VMCD) and Current-mode Class D (CMCD) power amplifiers. CMCD power amplifier behaves like a current source, i.e. amplifier's output voltage modulates with reactive load. Whereas in a properly working outphasing scheme, the output voltage of an amplifier should follow the phase of the input signal and the output current should be modulated by the load. It is therefore an unsuitable candidate for amplification with non-isolating combiners.

Figure 2.2 illustrates circuit schematic and output current/voltage waveform for VMCD PA. The active devices configured in push-pull mode are driven by 180° out-of-phase constant envelope signals. When Q1(pMOS) is on, Q2(nMOS) turns off and output voltage equals supply voltage. Likewise, output is zero when Q1 is switched-off and Q2 is operating in on-state. Output signal is passed through a series tuning circuit resonating at fundamental frequency to filter all harmonic

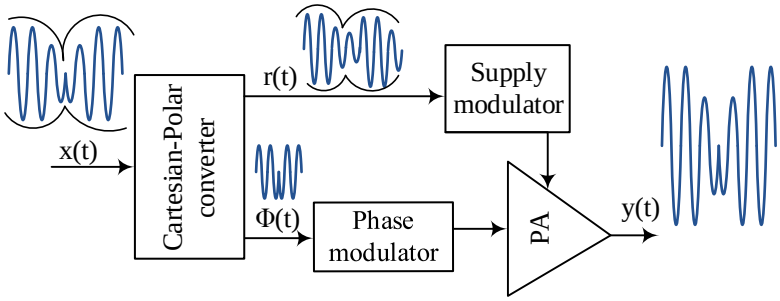

Figure 2.3: Conventional Polar architecture.

content. The VMCD PA behaves like an ideal voltage source, V_{out} is regulated by the input driving signal.

Class E PA utilizes a transistor, tuning circuit and reactive impedance components to minimize overlap between current and voltage waveforms. It is a intermediary topology between pure switch-mode and linear PA classes. Class E achieves high efficiency only if the transistor sustains small current during off-state, small voltage drop in on-state and small switching time compared to waveform period. Its output waveform is analog in shape, its mode of operation can be supported by a transistor with slower switching characteristics and is better suited to high frequency operation [11]. Existing Class E power amplifiers implementations perform high efficiency amplification up to K-bands [3], [12].

Class F power amplifiers also use a single transistor which is terminated with a load network. Ideally Class F V_{out} waveform is a square-wave and output current is a half-sinusoid. Load network shapes the transistor output waveforms, it provides low impedance to all the even harmonics and high impedance to odd harmonics. Class F current voltage relationship is similar to Class D power amplifier for an infinite number of harmonics [9],[10],[13].

Conventional power amplifiers are linear devices, but they exhibit high nonlinearity in order to achieve efficient operation. Likewise, Switch-mode PAs are efficient yet inherently non-linear devices. Efficient PAs serve as a bottle neck in the design of transceivers by limiting maximum achievable data rate. Thus, transmitter architectures designed to accommodate non-linear power amplifiers, for efficient amplification of high PAPR signals, are required to facilitate implementation of next generation transceivers.

2.2 Next Generation Transmitters

Power amplifiers significantly contribute towards efficiency and linearity of wireless transmitters. Efficient power amplifiers create a significant amount of distortion for varying envelope signals. Consequently, conventional Cartesian transmitters can't

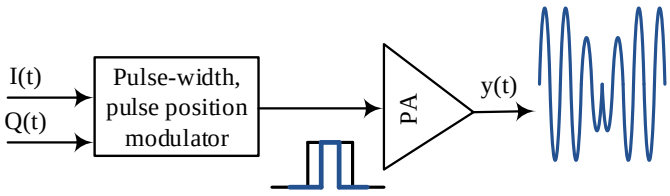

Figure 2.4: Pulse-width pulse-position modulated transmitter architecture.

satisfy the spectral emission requirements with these PAs.

Polar transmitters can benefit from non-linear PAs, as they transform the base-band signal into polar form to process amplitude and phase components along separate paths. The Polar architecture is shown in Fig. 2.3, where the amplitude $r(t)$ modulates the PA supply voltage through a DC-DC converter, and the phase modulated signal drives the PA.

Polar modulators achieve high average efficiency over a broad range of PA output power [5]. However, polar transmitters are not suitable for wideband transmission, as efficiency of the power converter degrades with the increase in bandwidth. This drawback further intensifies due to the 5-10 times bandwidth expansion caused by non-linear conversion operation from Cartesian-to-polar coordinates in outphasing transmitters [14]. The structural difference between high frequency (driving signal) and low frequency (envelope) signal paths creates difficulty in accurate delay matching. Differential delay and finite envelope bandwidth will result in phase mismatch, creating intermodulation distortion in the output signal. Furthermore, multiplication of amplitude and phase signals in the power amplifier results in convolution of the spectra in frequency domain. It introduces unwanted in-band and out-of-band spectral components. PA supply modulation will also introduce V_{DD}-AM and V_{DD}-PM distortion [15].

Pulse-width pulse position modulated (PWPM) PA architecture can also deploy a non-linear PA in a linear manner. It modulates PA output amplitude by varying the pulse width of the driving signal, and the position of pulses encodes phase information of the transmitted data [16],[17]. PWPM achieves high efficiency operation, but it exhibits constrained o/p signal dynamic range for high PAPR signals. As it is difficult to produce narrow pulses at GHz range, furthermore these pulses could be filtered out by transmitter components [5].

Outphasing amplifier decomposes a signal into two constant envelope signals. These signals are up-converted and amplified using SMPAs to be combined before transmission. This scheme does not possess any of the above mentioned limitations for wideband or high PAPR signals, making it suitable for amplification of these signals as will be discussed in the following section.

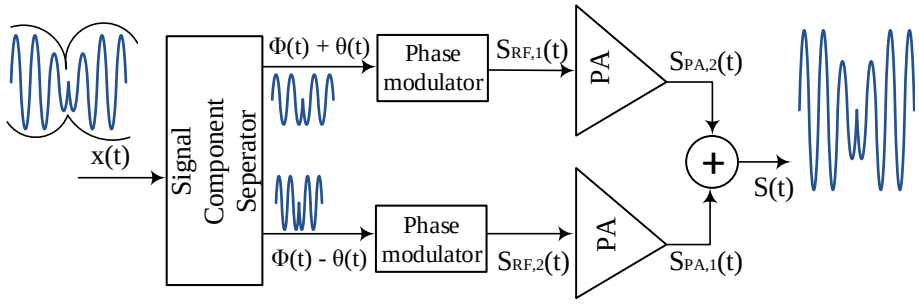

Figure 2.5: Outphasing transmitter.

2.3 Outphasing Concept

Outphasing concept was presented by Chireix in 1930s to improve AM broadcast transmitter performance [18]. It was later reinvented to realize linear amplification using non-linear components (LINC) for intermediate RF PA stages [19]. The basic principle of outphasing amplification is to decompose a signal having both amplitude and phase modulation into two constant envelope phase-modulated (PM) signals such that their vector sum reproduces the input signal. These PM signals are then passed along symmetric RF paths, each employing modulators and power amplifiers for up-conversion and amplification. PA output signals are summed up at the combiner to acquire an amplified version of the input signal. The outphasing transmitter architecture is illustrated in Figure 2.5. The signal component separator (SCS) input signal, in polar form, is given as

$$x(t) = \alpha(t)e^{j\phi(t)},$$

here $\alpha(t)$ denotes input signal amplitude modulation and $\phi(t)$ denotes phase modulation. The baseband signal $x(t)$ is applied to SCS, which modifies $x(t)$ into two constant envelope signals. The outphasing signals are generated using the phase angle of the input signal, $\phi(t)$, and the outphasing angle $\theta(t)$, which is formulated as

$$\theta(t) = \arccos \frac{\alpha(t)}{\alpha_{max}}. \tag{2.1}$$

The RF phase modulated outphasing signals are expressed as

$$S_{RF,1}(t) = \alpha_o cos(w_c t + \phi(t) + \theta(t))$$
$$S_{RF,2}(t) = \alpha_o cos(w_c t + \phi(t) - \theta(t)),$$

here α_o is a constant equal to $\alpha_{max}/2$. These RF PM signals are amplified and summed up at the combiner to produce an amplified (by a gain factor G) version of

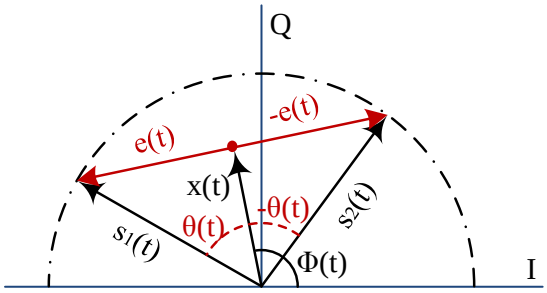

Figure 2.6: Vector diagram for Outphasing concept.

the input signal $x(t)$, given as

$$S_{OUT} = S_{PA,1}(t) + S_{PA,2}(t) = 2G\alpha(t)cos(w_c t + \phi(t)).$$

Phase difference between $S_{RF,1}(t)$ and $S_{RF,2}(t)$ determines the combined signal amplitude level. When $S_{RF,1}(t)$ and $S_{RF,2}(t)$ are in-phase, they add constructively to produce large amplitude signal at the combiner output. Likewise, anti-phase outphasing signals generate small amplitude levels by canceling each other at the combiner output [20]. The quadrature signal $e(t)$ is responsible for input signal decomposition in the SCS. The mathematical expression of $e(t)$ is a useful tool for understanding and analysis of the outphasing concept. It can be observed from Fig. 2.6, illustrating outphasing signal vector decomposition, that

$$e^2(t) = |s_1^2(t)| - |x^2(t)|,$$

where $s_1(t)$ is the complex envelope of $S_{RF,1}(t)$. The maximum amplitude of the input signal is α_{max}, yielding

$$|e(t)| = \sqrt{\alpha_{max}^2 - |x^2(t)|}.$$

The quadrature signal $e(t)$ is perpendicular to $x(t)$, thus it can be mathematically expressed as

$$e(t) = jx(t)\sqrt{\frac{\alpha_{max}^2}{\alpha^2(t)} - 1}. \tag{2.2}$$

The complex envelope of the phase modulated signals, $s_1(t)$ and $s_2(t)$, are therefore given as

$$s_1(t) = x(t) + jx(t)\sqrt{\frac{\alpha_{max}^2}{\alpha^2(t)} - 1} \tag{2.3}$$

$$s_2(t) = x(t) - jx(t)\sqrt{\frac{\alpha_{max}^2}{\alpha^2(t)} - 1}. \tag{2.4}$$

Hence, outphasing transmitter has the potential to linearly and efficiently amplify varying envelope signals, given that the two branch signals are perfectly balanced. The outphasing scheme is fundamentally linear as the constant envelope signal does not suffer from distortions caused by PA non-linearity. The use of non-linear power amplifiers drastically improves power amplifier efficiency, which contributes towards overall transmitter performance. However, outphasing transmitter efficiency depends on many factors besides the PAs. These factors are discussed in the following section.

2.4 High Efficiency Outphasing Techniques

Outphasing transmitter has potential for efficient and linear amplification of wideband high PAPR signals. Its performance heavily depends on the choice of power amplifier and power combiner utilized, as well as the signal dynamics.

Conventional outphasing architecture (LINC) uses isolating power combiners (Wilkinson combiner or hybrid coupler) to meet linearity requirements of wireless standards. These matched combiners realize highly linear operation by providing isolation between input ports. During summation, constructively-summed power is delivered to the antenna and residual power is delivered to the isolation resistor/port, to be dissipated as heat. When the outphased signals are in-phase, a small amount of power is wasted during signal combining, and the amount of dissipated power increases as the phase difference between outphased signals increases. In effect, average efficiency of LINC transmitter degrades significantly for signals exhibiting high PAPR. The instantaneous efficiency of isolating combiners is a function of the outphasing angle $\theta(t)$,

$$\eta_{Comb} = cos^2(\theta(t)).$$

PAs driven by constant envelope signals consume a fixed amount of power at all times. If a RF PA exhibits 100% efficiency and the passive combiner has zero contribution towards transmitter power budget, LINC efficiency is directly proportional to the power delivered to the antenna, expressed as

$$\eta_{Avg} = \eta_{Amp} \int_0^{\frac{\pi}{2}} p(\theta) cos^2(\theta) d\theta.$$

Here, η_{Amp} - the average PA efficiency - equals 1 and $p(\theta)$ is the probability density function (PDF) of the input signal at each outphasing angle $\theta(t)$. Isolating combiners achieve 100% efficiency only for the maximum output power level, and power efficiency degrades with phase difference between branch signals [21]. Hence time-average efficiency of conventional LINC is inversely proportional to the PAPR of the transmitted signal. A significant amount of power is wasted in isolating combiners,

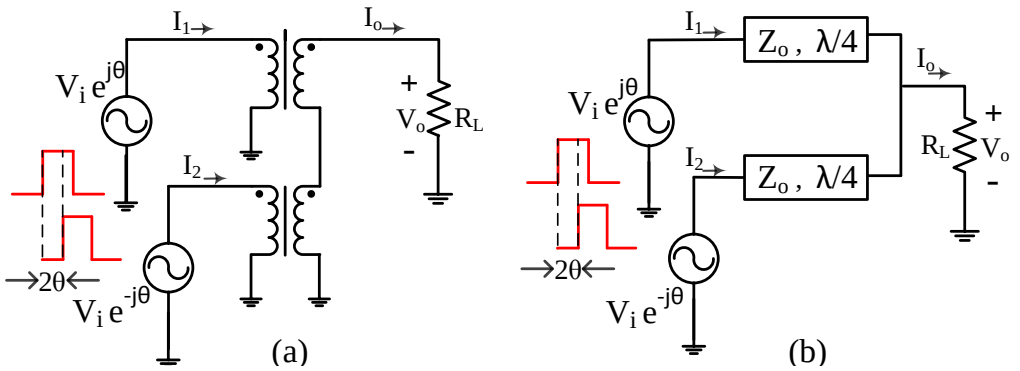

Figure 2.7: (a) Outphasing TX with transformer combiner. (b) Outphasing TX with Transmission-Line combiner.

making them unsuitable for efficient amplification of high PAPR signals [2],[5].

2.4.1 Non-isolating Combiner

Isolating combiners (Wilkinson combiner or hybrid coupler) provide a fixed port impedance which is matched to the PA output impedance in order to minimize reflections. This fixed load impedance draws a constant current from the PAs, and as a result outphasing transmitter efficiency is inversely proportional to the PAPR of the transmitted signal.

Lossless combiners alleviate the problem of efficiency degradation in isolating combiners by providing a time-varying load impedance. This load variation has the potential to significantly improve outphasing transmitter efficiency. Power amplifiers see a modulated load impedance which is a function of the outphasing angle $\theta(t)$. As a result, the PA output current and DC power consumption also scale with $\theta(t)$. Efficiency of the outphasing transmitter remains high regardless of outphasing angle, and high PAPR signals can be combined in an efficient manner [2]. Transmission-Line (TL) and transformer combiners are classified as unmatched non-isolating combiners.

Outphasing transmitter with the transformer combiner is shown in Figure 2.7a. Voltage sources represent ideal switch-mode power amplifier behavior. It can be seen that transformer secondary winding current is common for all PAs. If turn ratio is considered 1:1 with perfect mutual coupling, the combiner output voltage (at fundamental frequency) is expressed as

$$V_o = \frac{4}{\pi} 2V_i cos(\theta).$$

Common phase modulation $\phi(t)$ for both branches has been ignored since it does not affect the analysis. Primary currents I_1 and I_2 are equal to the secondary output

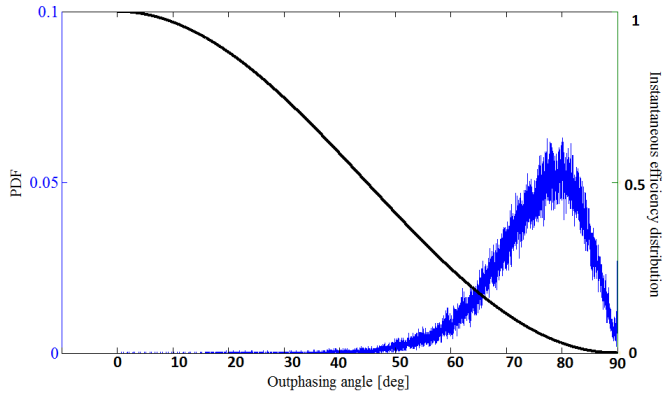

Figure 2.8: PDF of a multi-carrier OFDM signal with 100 MHz aggregated bandwidth and instantaneous combiner efficiency for Hybrid/TL/transformer combiners.

current I_o, given as

$$I_o = I_1 = I_2 = \frac{4}{\pi}\frac{2V_i cos(\theta)}{R_L}. \tag{2.5}$$

Fig. 2.7b illustrates outphasing architecture with the quarter-wavelength transmission line, a T-junction and ideal PAs. The fundamental frequency component of V_o equals

$$V_o = -j\frac{4}{\pi}\frac{2R_L V_i cos(\theta)}{Z_o},$$

where Z_o is the characteristics impedance of the transmission line. I_1 is equal to I_2 and I_o, defined as

$$I_o = I_1 = I_2 = \frac{4}{\pi}\frac{2R_L V_i cos(\theta)}{Z_o^2}. \tag{2.6}$$

The power amplifier output currents I_1 and I_2 vary with outphasing angle $\theta(t)$ in both non-isolating combiner types. If RF power amplifiers behave like ideal voltage sources, amplifier output voltage is independent of output current. Combiner output voltage is the sum of PA voltages and is independent of load impedance, thereby LINC is a linear transmitter [22],[13].

Instantaneous combiner efficiency curve follows a $cos^2\theta$ distribution for isolating, transmission-line and transformer combiners. Figure 2.8 shows that the instantaneous combiner efficiency maximum occurs at zero outphasing angle. Multi-carrier signals exhibit high PAPR, and as a result the distribution of outphasing angle $\theta(t)$

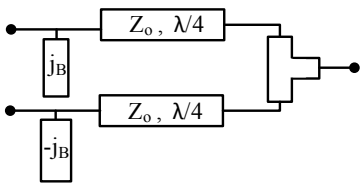

Figure 2.9: Chireix outphasing combiner.

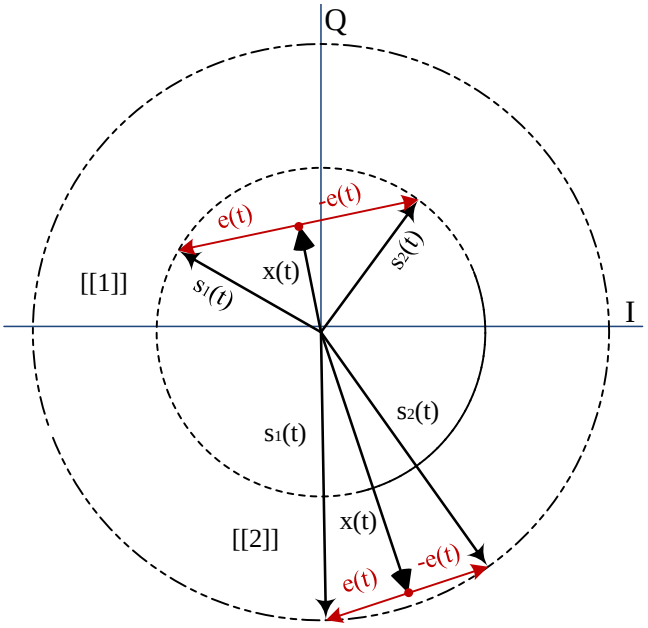

Figure 2.10: Outphasing vector diagram of MLINC scheme (1 amplitude bit) for two sampling instants.

is uneven with high occurrence of angles close to 90^o. This opportunity for efficiency optimization is exploited in *Chireix combiners*. Chireix combiners are composed of quarter-wavelength transmission lines, a tee junction and shunt reactance (of opposite values) at the input of each transmission line, as shown in Fig. 2.9.

Chireix combiner instantaneous efficiency can be expressed in compact form as [23]

$$\eta_{inst} = K cos^2(\theta - \gamma), \tag{2.7}$$

where, K is constant for a given combiner configuration, depending on the characteristic impedance of the transmission lines and the stub length. Equation (2.7) demonstrates that the instantaneous efficiency curve for the Chireix combiner shifts by an amount equal to electrical stub length γ. Thus, LINC combiner average efficiency can be improved by introducing suitable stub lengths to translate it's instantaneous efficiency curve to regions of high probability of $\theta(t)$ [1], [2].

2.4.2 Multi-level LINC

Multi-level linear amplification with non-linear components (MLINC) is an extension of a conventional outphasing architecture. It utilizes multiple amplitude levels to represent the outphased signals $S_{RF,1}(t)$ and $S_{RF,2}(t)$.

In conventional LINC, a small signal level at combiner output $S_{out}(t)$ is attained by generating outphased signals with a large phase difference. The same combined output level in MLINC is generated with smaller amplitude levels of $S_{RF,1}(t)$ and

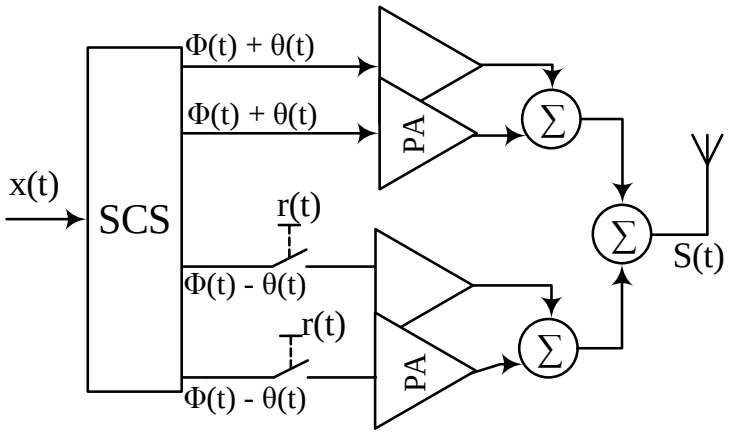

Figure 2.11: MLINC architecture for 1 amplitude bit (2 amplitude levels).

$S_{RF,2}(t)$ [5]. As shown in Fig. 2.10, the magnitudes of the outphased signals are small for the small input signal $x(t)$ at the sampling instant [[1]].

Since the quadrature signal power is dissipated during summation, MLINC achieves higher efficiency than conventional LINC by dividing α_{max} into multiple α_s [24]. The quadrature signal for MLINC transmitter is expressed as

$$e'(t) = jx(t)\sqrt{\frac{\alpha_s^2}{\alpha^2(t)} - 1}.$$

In MLINC transmitters, the ratio of the peak power to the instantaneous power, $\alpha_s^2/\alpha^2(t)$, is closer to 1 than in LINC (on average). The quadrature signal power is therefore smaller, and MLINC is thus expected to be less sensitive to mismatches along the phase modulated signal paths. This will be assessed with extensive simulations in Chapter 4.

MLINC architecture achieves higher power efficiency for a given combiner by reducing the average outphasing angle $\theta_{avg}(t)$, and by using smaller supply voltages in the PA's. The latter can be achieved either by supply voltage modulation [21] or by having parallel PA pairs with smaller supply voltages. MLINC operation achieved through PA supply modulation results in supply-voltage induced (V_{dd}-AM and V_{dd}-PM) distortion in the PA output signal, and may severely damage signal integrity and OT linearity [25].

This study analyzes MLINC architecture shown in Fig. 2.11. MLINC scheme (1-amplitude bit) consists of two pairs of PAs each driven by phase modulated signals $S_{RF,1}(t)$ and $S_{RF,2}(t)$. For low output signal level, one PA pair performs amplification, while the other pair is active only for high output amplitude levels.

3. LINEARITY OF OUTPHASING TRANSMITTER

Outphasing transmitter decomposes an amplitude and phase modulated signal into two phase modulated signals. These signals are passed along congruent RF paths for amplification using highly efficient non-linear PAs and combined to obtain amplified version of input signal. Outphasing architecture linearity depends on the matching of these RF paths. The non-linear conversion from Cartesian-to-polar coordinates expands the spectrum of phase modulated signals beyond the desired bandwidth limit. Linearity of outphasing amplifier is subject to exact cancellation of the wideband signal components at the combiner. A slight mismatch between RF paths might cause in-complete cancellation of the quadrature signal; creating in-band distortion as well as out-of-band interference [26]. Adjacent Channel Leakage ratio (ACLR) quantifies out-of-band (OOB) spectral re-growth caused by transmitter non-linearity, and it is used as the main figure-of-merit in this thesis. It is defined as the ratio of filtered mean transmitted power on the allocated channel frequency to the filtered mean received power present in the adjacent channel [27]. These imperfections and their impact on outphasing transmitter linearity will be reviewed in the following sections.

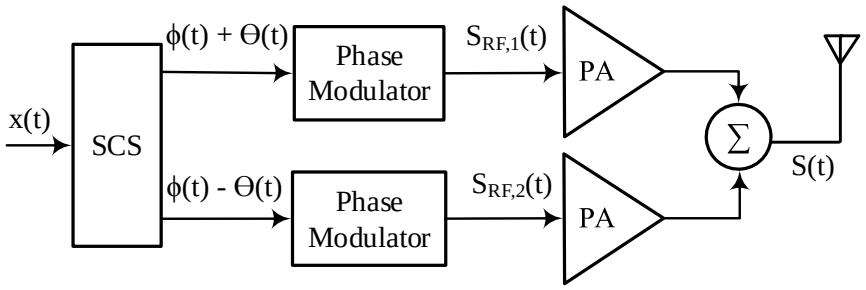

Figure 3.1: Outphasing transmitter architecture.

Figure 3.1 shows outphasing architecture analyzed in terms of ACLR for various imbalances and practical circuit impairments. Baseband signal $x(t)$ is passed along Signal Component Separator (SCS) to calculate the signal phase $\phi(t)$ and the outphasing angle $\theta(t)$. The phase signals are used to modulate the phase of the LO signal, producing the two phase modulated signals, $S_{RF,1}(t)$ and $S_{RF,2}(t)$. These

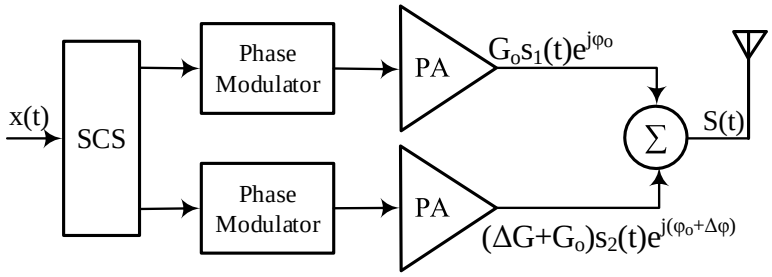

Figure 3.2: Baseband model of outphasing transmitter under path mismatches.

branch signals are amplified and summed at the combiner before transmission.

Practical outphasing transmitters suffer from distortion created as a result of several non-ideal effects and imperfections introduced by it's components. These imperfections include: IQ-modulator mismatches, gain, phase and timing/delay mismatch between branch signals, power amplifier imperfections and combiner induced non-linearity. These imperfections and their impact on outphasing transmitter linearity will be reviewed in the following sections.

3.1 Path Imbalance

Gain and phase imbalance between PA branches in outphasing amplifiers collectively represents path imbalance. The parallel branch scheme in this architecture leads to a small tolerance window for mismatches between paths, in order to limit out-of-band spectral regrowth. Path mismatch is mainly contributed by gain and phase characteristic mismatch between branch PAs. Though power combiner, PA matching network and biasing circuit non-linearities may also contribute towards it. The non-ideal behavior of various blocks itself stems from fabrication process tolerances of transistors and temperature difference [26]. Therefore, outphasing transmitters exhibit unavoidable path imbalance. It directly affects the linearity performance of transmitters. Fortunately, the scope of path imbalance for amplifiers, driven by constant envelope signals, is limited to amplitude and phase imbalance.

The effect of path imbalance on OT performance is analyzed as follows. Consider two branch (0 amplitude bit) outphasing amplifier in Fig. 3.2, intrinsic gain and phase of the two amplifiers is G_o and ϕ_o, and mismatch of ΔG and $\Delta\phi$ between them. The complex envelope of the combiner output signal is expressed as

$$\begin{aligned} s_{out}(t) &= G_o e^{j\phi_o}[x(t)-e(t)] + G_o(1+\frac{\Delta G}{G_o})e^{j(\phi_o+\Delta\phi)}[x(t)+e(t)] \\ &= G_o e^{j\phi_o}\Big(\big[1+\big(1+\frac{\Delta G}{G_o}\big)e^{j\Delta\phi}\big]x(t) + \big[(1+\frac{\Delta G}{G_o})e^{j\Delta\phi}-1\big]e(t)\Big) \quad (3.1) \\ &= G_1 x(t) + G_2 e(t). \end{aligned}$$

If the assumed imbalances $\frac{\Delta G}{G_o} << 1$ and $\Delta\phi << 1$ rad, the reference signal $s(t)$ will be scaled by complex constant

$$G_1 = [1 + (1 + \frac{\Delta G}{G_o})e^{j\Delta\phi}] \approx 2,$$

and the quadrature signal, $e(t)$ by

$$G_2 \simeq [1 + j\Delta\phi + \frac{\Delta G}{G_o} - 1] = (j\Delta\phi + \frac{\Delta G}{G_o}).$$

Normalizing $s_{out}(t)$ to $G_o e^{j\phi_o}$, (3.1) becomes

$$s_{out}(t) = 2x(t) + e(t)(\frac{\Delta G}{G_o} + j\Delta\phi). \tag{3.2}$$

As is evident from (3.2), amplitude and phase imbalance gives rise to an uncanceled quadrature signal term at the combiner output. This term creates both in-band distortion and out-of-band signal re-growth in outphasing transmitters.

The effect of path imbalance on the linearity of outphasing transmitters can be quantified through ACLR. It is the ratio of transmitted power in the desired band to out-of-band (OOB) power received in the adjacent channel [27]. Assuming input signal $x(t)$ to be band-limited i.e. it has negligible power outside the band of interest. ACLR for outphasing transmitter with path imbalance is analytically expressed as

$$ACLR(dB) = \frac{\int_{Fc-\frac{BW}{2}}^{Fc+\frac{BW}{2}} S_{OUT}(f)\,\mathrm{d}f}{\int_{Fc-\frac{BW}{2}+\Delta F}^{Fc+\frac{BW}{2}+\Delta F} S_{OUT}(f)\,\mathrm{d}f}. \tag{3.3}$$

Integral limit is defined by carrier frequency F_c, signal bandwidth BW, and channel spacing between reference channel and adjacent channel ΔF. The integral limits can be represented in concise form by R and A, R symbolizes the frequency region of the reference channel and A depicts the frequency region of the adjacent channel. Substituting $S_{OUT}(f)$ from (3.2) in (3.3),

$$ACLR(dB) = 6.02 - 20\log_{10}\left|\left(j\Delta\phi + \frac{\Delta G}{G_o}\right)\right| + 10\log_{10}\left[\frac{\int_R |X(f)|^2\,\mathrm{d}f}{\int_A |S_{OUT}(f)|^2\,\mathrm{d}f}\right]. \tag{3.4}$$

In multilevel outphasing transmitters, the ratio of peak power (at a given amplitude level) to instantaneous power, $\alpha_{max}^2/\alpha^2(t)$ is on average closer to 1 than in LINC. Based on (3.2), the quadrature signal power, and therefore the sensitivity of multi-level OT to mismatches, is expected to be smaller. This will be verified through simulations in Chapter 4.

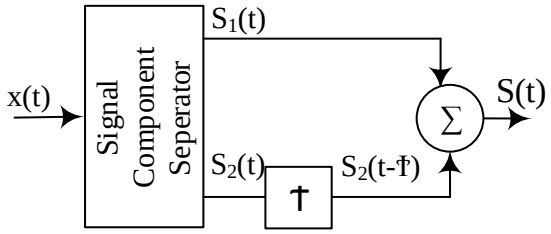

Figure 3.3: Delay mismatch in outphasing transmitter.

3.2 Delay Imbalance

Delay mismatch is a constant propagation time difference between the outphasing branch signals. In integrated circuits, signal propagation delay variation originates from fabrication process variations. These variations particularly influence circuit performance in deep sub-micron technologies. Delay imbalance is contributed by blocks following the SCS in outphasing transmitters [28]. Figure 3.3 illustrates an outphasing amplifier with delay imbalance τ between outphased branches. The complex signal at combiner output under delay imbalance is expressed as

$$s_{out}(t) = \; x(t) + e(t) + x(t-\tau) - e(t-\tau). \tag{3.5}$$

Delay mismatch gives rise to incomplete cancellation of quadrature signal at the combiner output, which produces out-of-band (OOB) signal re-growth and in-band distortion in outphasing transmitters. Rearranging (3.5),

$$s_{out}(t) = x(t)\left(1 + j\sqrt{\frac{\alpha_{max}^2}{\alpha^2(t)} - 1}\;\right) + x(t-\tau)\left(1 - j\sqrt{\frac{\alpha_{max}^2}{\alpha^2(t-\tau)} - 1}\;\right). \tag{3.6}$$

Delay mismatch can be approximated in the vicinity of the carrier frequency F_c in terms of a phase mismatch $\Delta\phi$, as

$$\tau = \frac{\Delta\phi}{2\pi F_c}. \tag{3.7}$$

Considering band-limited input signal $x(t)$ i.e. it has negligible power outside the band of interest. From (3.3) and (3.7), ACLR for outphasing transmitter under the influence of delay imbalance is expressed as

$$ACLR(dB) = 6.02 - 20\log_{10}\left|j\tau w_c\right| + 10\log_{10}\left[\frac{\int_R |X(f)|^2\,\mathrm{d}f}{\int_A |S_{OUT}(f)|^2\,\mathrm{d}f}\right], \tag{3.8}$$

where the integral limit R and A are the frequency regions of the reference channel and the adjacent channel, respectively.

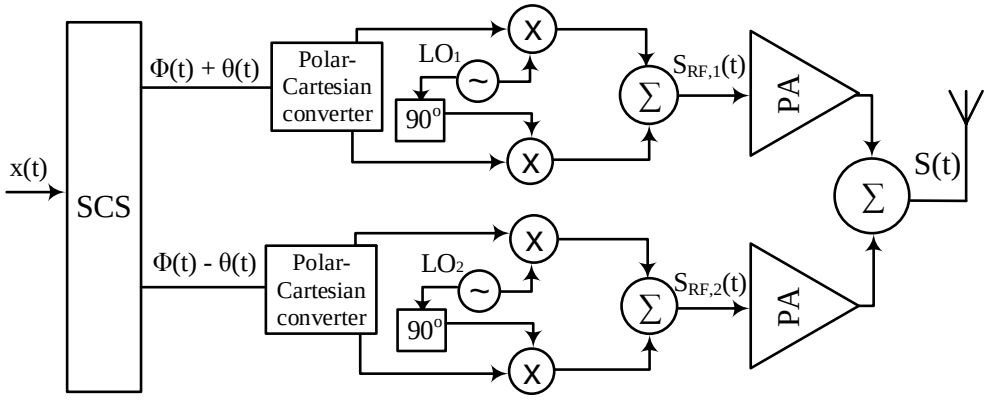

Figure 3.4: Outphasing transmitter (LINC) with IQ modulator based up-conversion.

3.3 Quadrature Modulator Mismatches

In-phase and quadrature modulator (IQ modulator) is a popular technique for modulating a baseband signal onto an RF carrier. In the outphasing transmitter context, digital data $s_k(t)$ from SCS is divided into two parallel data streams, termed as I and Q channels. I- and Q- branch signals are real valued signals evaluated as

$$\begin{aligned} I_k &= Re[s_k(t)] \\ Q_k &= Im[s_k(t)], \end{aligned}$$

$k = 1, 2$ denotes the IQ modulator in the respective outphasing branches. I/Q channel data is modulated to radio frequency through two identical local oscillator (LO) signals with phase difference of 90^o. Then, these channels are added to acquire the phase modulated RF signals $S_{RF,k}(t)$ as illustrated in Fig. 3.4. The IQ modulated outphasing signal $S_{RF,k}(t)$ is mathematically expressed as

$$S_{RF,k}(t) = I_k cos(2\pi F_c t) - Q_k sin(2\pi F_c t).$$

Practical IQ modulators introduce errors in the transmitted data owing to several misalignments. Data symbols in I and Q channels will encounter different path gains, and phase shifts (due to imperfect LO phase shifter). Additionally, LO leakage and DC offset error effects will result in appearance of unmodulated RF carrier in the up-converted data signal [29]. These misalignments are prominent in outphasing transmitters, as they impact transmitter performance on two levels: errors caused within IQ modulators, and the relative mismatches between modulated branch signals.

Each I/Q branch signal will experience distinct gain and phase shift, with addition of unmodulated carrier signal. This difference of operation between I/Q channels can be modeled using parameters: differential gain g_d and differential phase shift ϕ_d

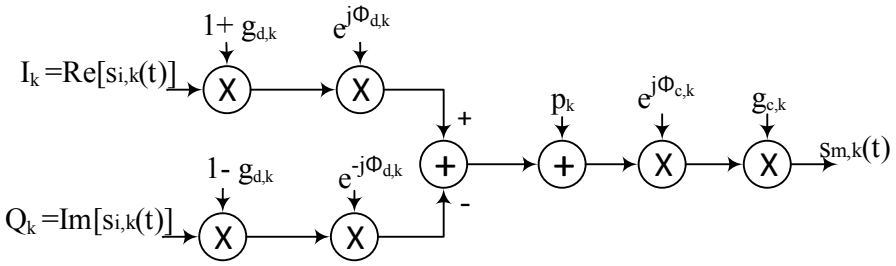

Figure 3.5: Baseband model of IQ modulator with differential misalignments g_d, ϕ_d and carrier leakage $p_{I/Q}$ [30].

between I and Q channels, and individual carrier offset $p_{I/Q}$. A graphical presentation of quadrature modulator misalignments is shown in Fig. 3.5. I- and Q-branch signals are offset by p_I and p_Q in their respective paths. Then, input signal is multiplied by gain constants $1+g_d$ and $1-g_d$, and modulated by carrier signal with phase difference of ϕ_d. The phase modulated signal with quadrature errors is expressed as

$$S_{RF,k}(t) = \big[(1+g_d)s_{I,k}(t)+p_I\big]cos(2\pi f_c t+\phi_d) \quad -\big[(1-g_d)s_{Q,k}(t)+p_Q\big]sin(2\pi f_c t-\phi_d). \tag{3.9}$$

Additionally, each outphasing branch will experience distinctive gain and phase shift, termed as common branch gain $g_{c,k}$ and common branch phase $\phi_{c,k}$ for each branch respectively. Representing $S_{RF,k}(t)$ in compact form, it's complex envelope $s_{m,k}$ is given by [31]

$$s_{m,k} = g_{c,k}e^{j\phi_{c,k}}u_k s_k + v_k s_k^* + p_k. \tag{3.10}$$

The constants in (3.10) are defined by [30]

$$\begin{aligned}
|u_k| &= \sqrt{cos^2\phi_{d,k} + g_{d,k}^2 sin^2\phi_{d,k}} \\
arg(u_k) &= atan(g_{d,k}tan\phi_{d,k}) \\
|v_k| &= \sqrt{g_{d,k}^2 cos^2\phi_{d,k} + sin^2\phi_{d,k}} \\
arg(v_k) &= atan(\frac{tan\phi_{d,k}}{g_{d,k}}) \\
p_k &= p_{I,k}cos(\phi_{d,k}) + p_{Q,k}sin(\phi_{d,k}) + j(p_{I,k}sin(\phi_{d,k}) + p_{Q,k}cos(\phi_{d,k})).
\end{aligned}$$

Equation 3.10 shows that the major effect of IQ modulator based errors is: unwanted amplitude modulation (AM) (due to the conjugate interference term $v_k s_k^*$), and phase distortion. The impact of IQ errors on performance of outphasing transmitter depends on the linearity of the power amplifier. An amplitude and phase modulated input signal will create intermodulation distortion in non-linear power amplifiers. Furthermore, IQ mismatches will result in incomplete cancellation of the quadrature signal $e(t)$ at the combiner output. Thus, IQ modulator errors will compromise the

linearity of outphasing transmitter for all power amplifier classes. The linearity performance of outphasing transmitter under IQ modulator mismatches, essentially depends on the amount of IQ errors (within each branch and between outphasing branches) and power amplifier nonlinearity.

3.4 PA Imperfections

RF power amplifier is the main amplifying stage in the transmitter that handles the highest level of RF power in the transmitter chain. Consequently, its characteristics heavily influence power efficiency and linearity of outphasing transmitters. Even though RF PAs are operated in a linear manner in outphasing transmitters i.e. driven by constant envelope signals, practical RF PA circuits introduce several non-linear effects.

Besides path imbalance, power amplifiers contribute towards the interference signal power at the combiner output through other non-linear effects. Traditional linear PAs (Class A, B, AB, C) utilize non-linear regions of operation in active devices (transistors) to achieve optimal efficiency. The non-linear characteristics of these amplifiers vary with process, temperature and load impedance. Though the branch PAs are utilized in linear fashion, they will create distortion at the combiner output owing to even slight differences in their non-linear characteristics. Linear class of PAs can be roughly characterized as memory-less weakly non-linear components. In this case, linear PA input-output characteristics can be represented by power series expansion, given as

$$S_k(t) = aS_{RF,k}(t) + bS^2_{RF,k}(t) + cS^3_{RF,k}(t)...$$

here, $S_{RF,k}(t)$ represents the modulated RF signal, a is the linear gain coefficient of the PA and b, c... -depict the component non-linearity, such as non-linearity introduced by power supply limitations. c represents the third-order PA characteristics responsible for the compression effect and intermodulation [3], [26]. Fortunately, higher order terms of power series expansion have little impact on characteristics of practical power amplifiers. Considering the first three terms of power series expansion, the PA output signals for first-order and third-order non-linearity (at the desired frequency) are approximated as

$$\begin{aligned} S_1(t) &\simeq a\Big[1 + \frac{3}{4}\frac{c_1}{a}S^2_{RF,1}(t)\Big]S_{RF,1}(t) \\ S_2(t) &\simeq a\Big[1 + \frac{3}{4}\frac{c_2}{a}S^2_{RF,2}(t)\Big]S_{RF,2}(t). \end{aligned} \tag{3.11}$$

Linear gain a is assumed to be the same for both power amplifiers. Mismatch in non-linear characteristics of PAs could create distortion at the combiner output.

This can be demonstrated, in the simplest manner, by expanding (3.11) for the ideal phase modulated input signals,

$$\begin{aligned} S_1(t) &\simeq a\Big[1+\frac{3}{8}\frac{c_1}{a}\alpha_o^2\Big]\alpha_o cos\big(w_c t+\phi(t)+\theta(t)\big) \\ S_2(t) &\simeq a\Big[1+\frac{3}{8}\frac{c_2}{a}\alpha_o^2\Big]\alpha_o cos\big(w_c t+\phi(t)-\theta(t)\big). \end{aligned} \tag{3.12}$$

The above expressions only show the PA output signal terms residing at the carrier frequency. PA nonlinearity with ideal phase modulated signals induces interference only if the PA nonlinear responses are different, in which case the effect is equivalent to a gain mismatch.

If the PA input signals are amplitude modulated by $g_k(t)$, the PA output signal from (3.11) is expressed as

$$\begin{aligned} S_1(t) &\simeq a\Big[1+\frac{3}{8}\frac{c_1}{a}g_1^2(t)\Big]g_1(t)cos\big(w_c t+\phi(t)+\theta(t)\big) \\ S_2(t) &\simeq a\Big[1+\frac{3}{8}\frac{c_2}{a}g_2^2(t)\Big]g_2(t)cos\big(w_c t+\phi(t)-\theta(t)\big). \end{aligned} \tag{3.13}$$

The amplitude modulation and the AM-AM distortions $g_k^3(t)$ will not be canceled upon combining, adding to the interference seen at the combiner output. Amplitude modulated input signal also creates AM-PM distortion in non-linear PAs, but the power series expansion cannot predict the combination of AM-AM and AM-PM conversion with real coefficients [32]. AM-AM and AM-PM conversion effects will be verified through simulations in Chapter 4.

Switch-mode power amplifiers drive transistors to operate as switches. The SMPA input signal is a square-wave signal generated in the driver amplifier stages. The driver stages may contribute towards slowing down the input signal of the PA switches. Moreover, realistic switch-mode waveforms possess a finite number of harmonics, owing to bandwidth limitations of preceding transmitter blocks. The finite rise- and fall-time of real world signals, results in PA input signals which are trapezoidal in nature. These realistic switch-mode waveforms create distortion in the outphasing transmitters [22], [33].

Furthermore, the non-ideal switching operation of SMPAs can also introduce distortion in the message signal. The finite switch resistance and parasitic gate-source capacitance C_{GS}, if not compensated, also creates distortion in the amplified signals. The finite switch resistance varies as a function of input signal voltage level, which could lead to AM-AM distortion in the combined signal. C_{GS} allows current to flow from the input to the output node during switching between voltage states, which adds undesirable phase-modulated signal at the output, and creates AM-PM distortion [15], [22], [24], [34].

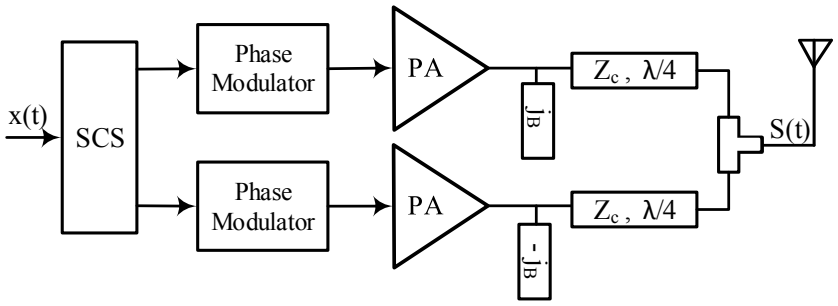

Figure 3.6: Chireix outphasing transmitter.

3.5 Combiner Induced Non-linearity

Power combiners generally fall into two categories: isolating (Hybrid) and non-isolating (transmission line, transformer and Chireix) combiners. Hybrid combiners provide good isolation between power amplifiers to ensure linear vector summation, but much of the efficiency inherited in outphasing transmitters is lost as the canceled power is dissipated as heat [35]. Moreover, the outphasing transmitter with an isolating combiner demonstrates high linearity only if RF paths are balanced and combiner is ideal [2]. These attributes advocates the use of unmatched non-isolating power combiner for outphasing transmitters.

As discussed in Section 2.4.1, non-isolating combiners ensure efficient operation by presenting time-varying load impedance to each branch PA. The load impedance R_L steers the DC current of the power amplifiers through the combiner output current I_o, as shown in Fig. 2.7. The output current of a non-isolating combiner is equal to the currents flowing through each input (PA) port, I_1 and I_2. The output voltage of the power amplifiers, V_1 and V_2 may depend on their respective output currents I_1 and I_2, and we get the following expression

$$I_o = I_1 = I_2 = \frac{V_1(I_o) + V_2(I_o)}{R_L}.$$

The output current interferes with PA functions which can lead to distortion at the combiner output. Moreover, the input ports of a lossless combiner are coupled, so the PAs affect the output of one another through the common output current I_o.

The interaction between branch amplifiers depends on the degree of influence I_o exhibits on the PA output voltage. Naturally, the choice of PA topology plays a critical role in transmitter linearity performance. As discussed in Section 2.1, voltage-mode Class D and Class F PA operation resembles voltage source behavior. Their output voltage is only controlled by the phase of the driving signal, making them a suitable candidate for the outphasing architecture [13].

In case of lossless combiners, it is not possible to simultaneously match all the

ports [36]. Impedance mismatch between the PAs and combiner input ports will cause reflections, which is the principle cause of linearity degradation in Chireix outphasing transmitters [37].

Chireix combiners introduce stubs to improve combiner efficiency by matching combiner input impedance and PA output impedance for a certain range of outphasing angles. The stub electric length is chosen in view of improving the average efficiency of OT. But, the added susceptance creates a significant amount of distortion for outphasing angles outside this range.

Fig. 3.6 shows a Chireix outphasing transmitter, the Chireix combiner consists of the two transmission lines having impedance Z_c, two stubs of susceptance B and a tee junction. The power amplifiers are assumed to be identical, having a real voltage gain G and an output impedance of Z_o. The expressions for the PA output signals and Chireix combiner output are derived in Appendix A. These expressions take into account the reflection effects caused by impedance mismatch between PA output and combiner input ports. From A.3, Chireix combiner output can be expressed as [23]

$$S_{OUT}(t) = \frac{2y\alpha_o G cos\gamma}{1 + 2y^2 cos^2\gamma} cos\big(w_c t + \phi(t)\big) cos\big(\theta(t) - \gamma\big). \tag{3.14}$$

The impedance mismatch, between the power amplifiers and the combiner input ports, introduces both amplitude and phase distortion in the output signal. Equation 3.14 can also be expressed in compact form as

$$S_{OUT}(t) = \alpha_o K G cos\big(w_c t + \phi(t)\big) cos\big(\theta(t) - \gamma\big). \tag{3.15}$$

Here, K is constant for a given Chireix combiner configuration. Since, the input signal from the power amplifier is $\alpha_o G cos(w_c t + \phi(t)) cos(\theta(t))$, the non-linearity of Chireix combiner can be quantified by the stub electrical length γ. If $\gamma = 0$ i.e. stubs are withdrawn, Chireix outphasing transmitter becomes a linear system.

Chireix combiners exhibit high efficiency, but they create a significant amount of in-band and OOB distortion in outphasing transmitters. Accordingly, the choice of power combiner plays a critical role in determining the transmitter's linearity and efficiency performance. Selection of the power combiner depends on the standard specifications for a certain outphasing transmitter application as well as the performance of the preceding blocks.

4. TX SIMULATIONS AND ANALYSIS

The outphasing transmitter (OT) is a good candidate for next generation transmitters; it can efficiently amplify high PAPR signals with good linearity. However, the phase modulated (PM) signals in OT have very wide bandwidth. This can be attributed to the quadrature signal $e(t)$, which is added to the message signal to obtain the constant envelope PM signals. The power spectrum of the phase modulated signals extends into the out-of-band region, interfering with signals in adjacent and alternate channels. For an ideal balanced transmitter, $e(t)$ signal power is canceled during recombination. Any mismatch or non-linearity encountered by the phase modulated signals will result in incomplete cancellation of the quadrature signal, creating in-band and out-of-band distortion. The propagation of wideband signals in congruent RF paths decreases the error tolerances in TX components, making linearity performance pivotal to commercialization of OT. Linearity performance of OT can be degraded by all component imperfections, which include limitations of digital signal processing, phase (IQ) modulator based errors, path/delay mismatches, power amplifier imperfections and combiner non-linearity.

4.1 Simulation Setup

Outphasing transmitter system-level model is utilized in this study to analyze its linearity performance for imbalances present in practical circuits. Its behavioral model was developed and analyzed in Matlab [38].

Fig.4.1 shows the outphasing transmitter model implementation in Matlab. OFDM symbols are generated using 64-QAM subcarrier modulation. The generated multi-

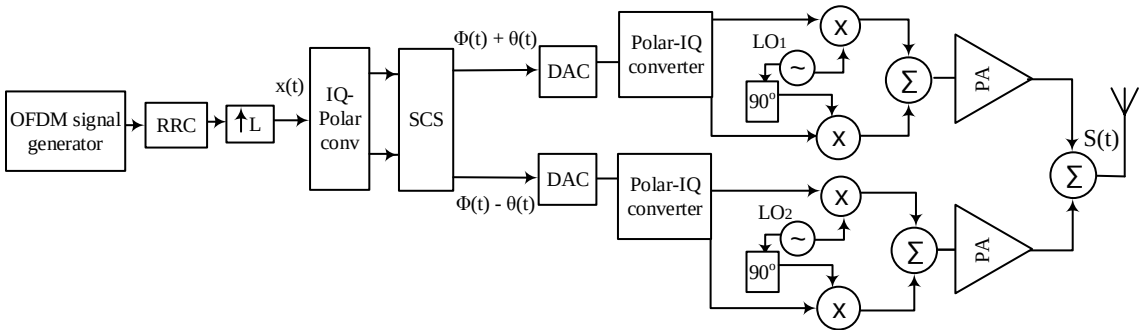

Figure 4.1: Outphasing transmitter implementation in Matlab.

carrier signal is an LTE downlink signal, consisting of 7 OFDM symbols - equivalent to 1 LTE slot. The OFDM symbols are windowed by a root-raised cosine window and interpolated to obtain the input signal $x(t)$. The digital baseband signal $x(t)$ is converted into polar form and processed in Signal Component Separator (SCS) to acquire the outphased signals. These signals are further oversampled using interpolators, which are used to model the digital-to-analog converters (DAC) in the simulator. Outphased waveforms are modulated to carrier frequency by IQ modulator based up-converter. The PM signals are amplified by linear (ideal Class A), non-linear or switch-mode power amplifiers. The non-linear amplifier is characterized by Ghorbani model, which matches well the practical AM/AM and AM/PM characteristics of the FET power amplifier [39]. Finally, the amplified signals from RF branches are recombined in the power combiner.

Carrier frequency of 2.5 GHz was set for all simulation results, the simulations include multiple single-carrier and aggregated carrier bandwidth cases. Graphs in the following sections include three single-carrier bandwidth (BW) cases: 5 MHz, 10 MHz and 20 MHz, and four aggregated-carrier bandwidth cases: 40 MHz, 60 MHz, 80 MHz and 100 MHz. According to the concept of relative bandwidth, the outphasing transmitter is regarded as a narrowband system for the simulated carrier frequency and bandwidth cases. Relative bandwidth is defined as [40], [41]

$$BW\% = \frac{F_H - F_L}{F_H + F_L} \times 200,$$

where, F_H and F_L are the upper and lower band edges of the signal respectively. Outphasing transmitter for largest bandwidth case (100 MHz) and carrier frequency (2.5 GHz) has relative bandwidth of 8%. A system with relative bandwidth less than 15% is generally considered as a narrowband system.

Out-of-band emissions are particularly affected by any imbalances encountered in the outphasing architecture. Residual power of $e(t)$ at the combiner output spreads into adjacent and alternate channels, creating distortion in out-of-band region. The undesired spectral regrowth around the carrier is measured by Adjacent Channel Leakage Power Ratio (ACLR), as defined in Section 3.1. Minimum allowable ACLR limit, defined by 3GPP [27], is 45 dB for LTE base station transmitter. This limit has been used as a benchmark for measuring maximum allowable imbalances in this study. The behavior of the outphasing transmitter for each imperfection is determined separately, to thoroughly investigate the performance limitations.

The following sections incorporate outphasing transmitter (0 amplitude bit resolution) and multilevel OT simulation results for sinusoidal and pulsed LO-waveform based phase modulation. Pulsed LO-waveform based results are exhibited exclusively for OT, because phase glitches occur in MLINC when switching between

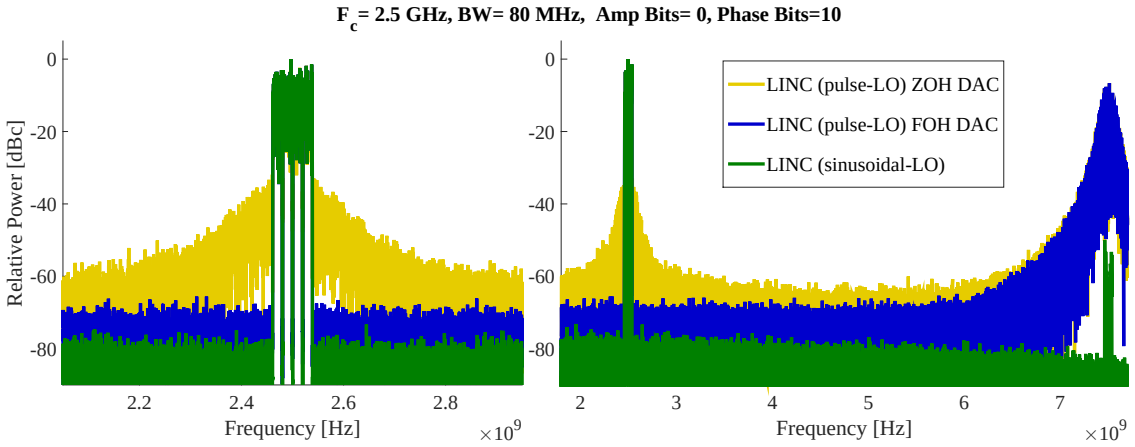

Figure 4.2: LINC spectra for sinusoidal and square-wave carrier based PM.

amplitude states, leading to broadening of the spectrum of the PM signals. This nonlinear content extends onto the desired and adjacent channels and limits the achievable ACLR (even without any mismatches).

The pulsed LO-waveform based phase modulation in outphasing transmitter is analogous to ideal switch-mode power amplification, and sinusoidal LO-waveform based phase modulation is analogous to ideal linear power amplification. Square-wave carrier based PM will be referred to SMPA and sinusoidal carrier based PM will be referred as Linear PA in the following sections.

4.2 Linearity of Square-Wave Carrier Based PM

Before proceeding with the analysis of OT linearity under mismatches, this study will shortly discuss the linearity performance limitations experienced in OT with square-wave carrier based phase (IQ) modulator. Outphasing transmitter with pulsed LO based phase modulator experiences higher distortion in comparison to its sinusoidal counterpart, which results from discrete-time signal processing of the outphasing signals $\phi(t) + \theta(t)$ and $\phi(t) - \theta(t)$. This fact is discussed in details below. The Fourier series expansion for a 50% duty-cycle square-wave carrier is

$$S_{LO}(t) = \sum_{n=1,3,5,..}^{\infty} \frac{4}{n\pi} cos(n(w_c t)). \tag{4.1}$$

The LO signal spectrum is composed of the local oscillator signal at the desired frequency and the odd-order harmonics, as seen in (4.1). LO signal is modulated with the outphasing signals to obtain,

$$S_{RF,k}(t) = \sum_{n=1,3,..}^{\infty} \frac{4}{n\pi} cos\big(n(w_c t + \Phi_k(t))\big), \quad \Phi_{k=1,2}(t) = \phi(t) \pm \theta(t).$$

The outphasing signals from DAC contain undesired spectral images at the multiples of the sampling frequency. These images are created due to sampling (interpolation) of the signal, and are insufficiently attenuated by the sample-and-hold operation. The phase modulated signal in the presence of spectral images

$$S_{RF,k}(t) = \sum_{n=1,3,..}^{\infty} \frac{4}{n\pi} cos\Big(nw_c t + n\big(\Phi_o(t) + \sum_i \Phi_i(t)\big)\Big) \tag{4.2}$$

here $\Phi_o(t)$ represents the baseband component of phase signal and $\sum_i \Phi_i(t)$ represents the sampling images at multiples of the sampling frequency. Expanding (4.2) to acquire [42]

$$S_{RF,k}(t) = \sum_{n=1,3,..}^{\infty} \frac{4}{n\pi}\Big(cos(nw_c t)cos\big(n\Phi_o(t) + n\sum_i \Phi_i(t)\big) - sin(nw_c t)sin\big(n\Phi_o(t) + n\sum_i \Phi_i(t)\big)\Big) \tag{4.3}$$

The DAC images (which are high with a zero-order hold (ZOH) DAC) mix with carrier harmonics (when PAs are highly nonlinear, e.g. switching) to create interference around the carrier, which decreases the signal-to-interference ratio. The spectra for outphasing transmitter with sinusoidal and square-wave carrier based phase modulators is shown in Fig. 4.2. There is ~24 dB difference in ACLR performance of both ideal transmitters for ZOH DAC. In order to improve performance of LINC scheme with square-wave carrier based PM, the results in the following sections are obtained for first order-hold (FOH) DAC, which was proposed in [42].

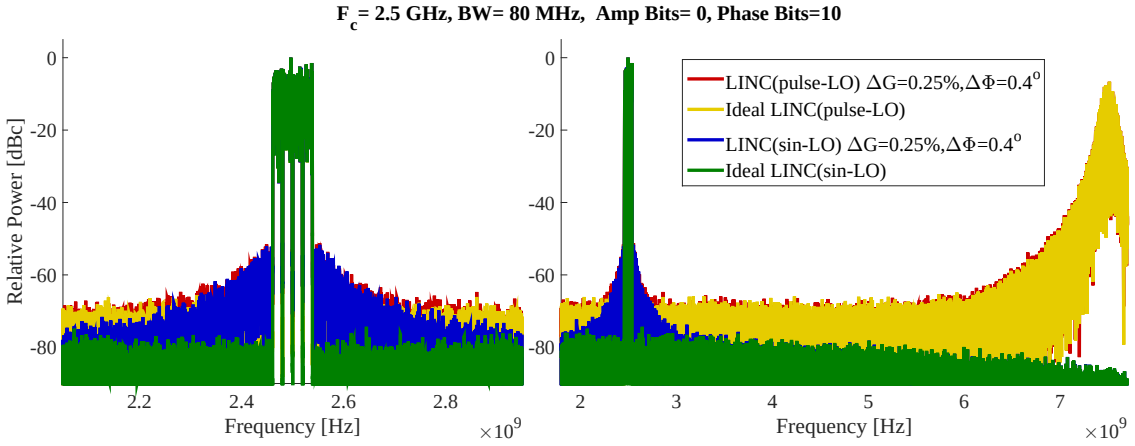

Figure 4.3: Spectra of LINC TX schemes with and without path imbalance: $\Delta G = 0.25\%, \Delta\Phi = 0.4^o$.

4.3 Path Mismatches

This section discusses linearity performance of outphasing transmitter for path imbalance. The linearity performance results of LINC and MLINC architecture for sinusoidal local oscillator (LO) based IQ modulator, and LINC results for pulsed-LO based IQ up-conversion are presented. The impact of path mismatch on LINC/MLINC is evaluated for an ideal transmitter architecture with only amplitude or phase mismatch between branch power amplifiers.

4.3.1 LINC Transmitter

Figure 4.3 illustrates outphasing transmitter output spectra for ideal and mismatched LINC scheme with pulsed and sinusoidal-LO based phase modulator. A perfectly linear LINC transmitter will utilize a sinusoidal LO waveform based phase modulator, Class A (linear) power amplifiers and isolated combiner. Adjacent channel leakage ratio (ACLR) for ideal LINC TX (green colored spectrum) is ~76 dB, which is mostly contributed by quantization noise. Path mismatches (amplitude mismatch of 0.25% and phase imbalance of 0.4^o) reduce ACLR to ~50 dB by introducing residual power of the quadrature signal $e(t)$ around the carrier frequency. OT spectrum (SMPA) introduces higher interference power (~67 dB ACLR) in adjacent

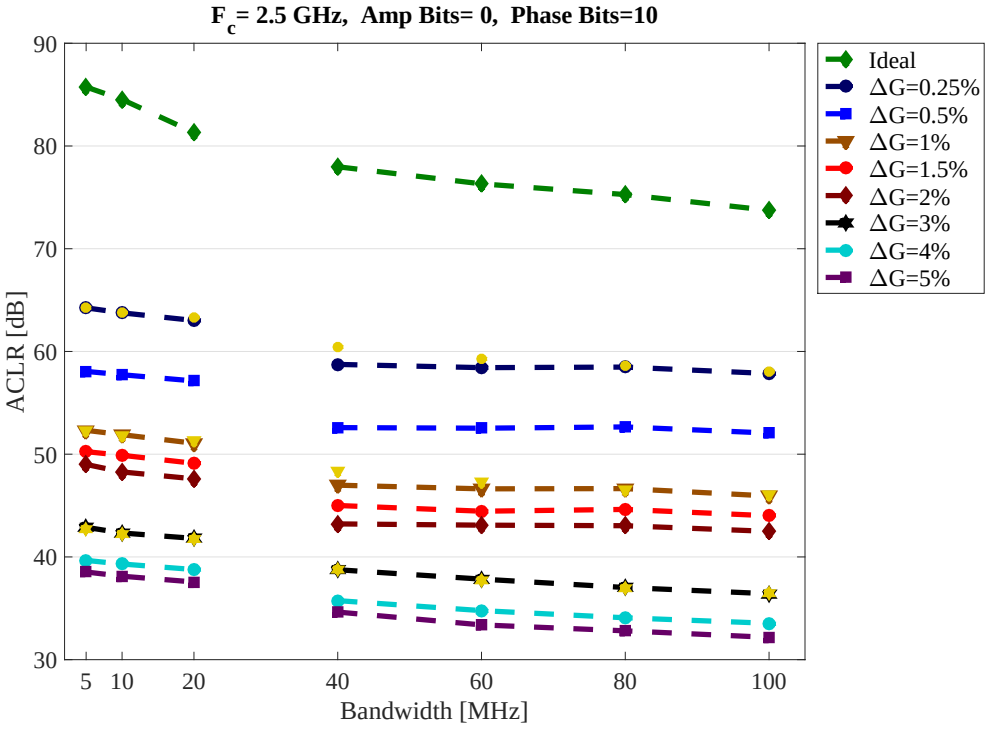

Figure 4.4: ACLR vs BW for (linear PA) LINC under amplitude imbalances, theoretical values (yellow dots) are evaluated for 0.25, 1, and 3% amplitude imbalances).

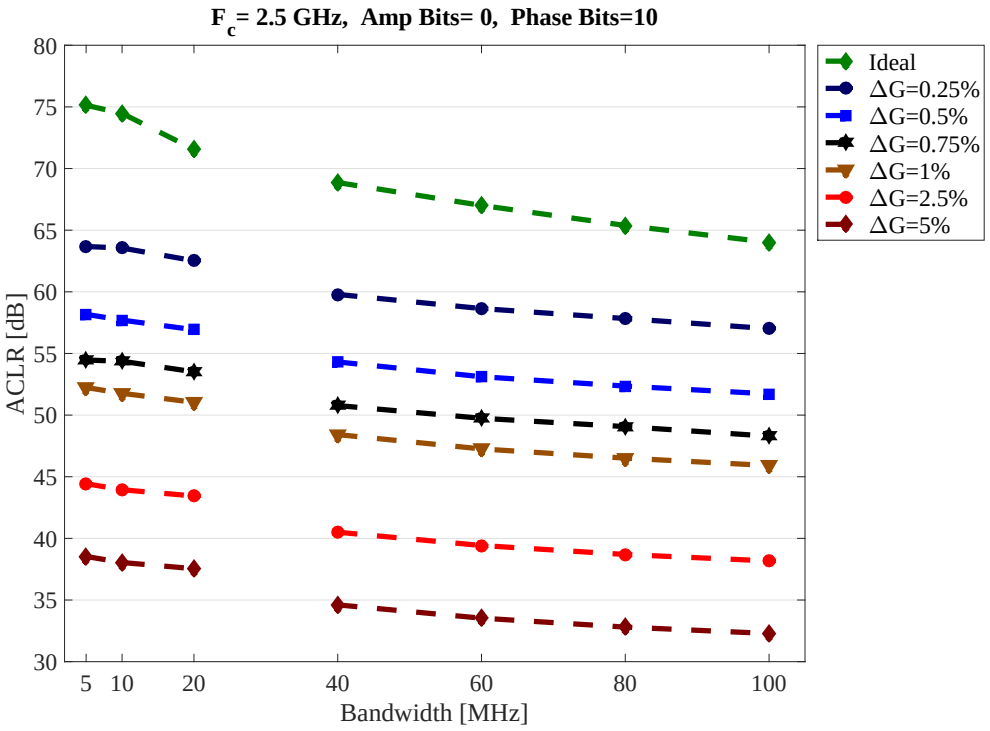

Figure 4.5: ACLR vs BW for (SMPA) LINC under amplitude imbalances.

channels, due to the mixing of DAC images with wideband odd-order harmonics. This scheme also exhibits ~50 dB ACLR under the specific path imbalance.

In Fig. 4.4, the amplitude imbalance is varied from 0.25% to 5% for LINC (Linear PA) scheme. The results are acquired for a 64-QAM OFDM signal of 10 bit phase resolution. ACLR performance curves for LINC are in good agreement with (3.4), the theoretical results are represented by yellow-colored symbols. The consistency of the two results indicates that linearity of the LINC scheme, under amplitude mismatch, is mostly influenced by the residual power of the quadrature signal $e(t)$. Carrier aggregated OFDM signals exhibit virtually constant ACLR for a given amplitude mismatch (between $\Delta G = 0.25$ to 2%) irrespective of signal bandwidth. Because, the residual amount of quadrature signal power at the combiner output essentially depends the quantity of amplitude mismatch between the branches. Though, $e(t)$ signal spectrum depends on input signal properties, such as bandwidth, its effect becomes apparent for larger amplitude imbalances (3% and above).

Figure 4.5 presents ACLR results for LINC (SMPA) scheme under amplitude imbalance range: 0.25% to 5%. The results for this scheme are comparable to the results acquired for LINC (Linear PA) TX, suggesting that amplitude mismatch considerably influences OOB distortion for (SMPA) LINC as well. As mentioned in section 4.1, these graphs represent performance of OFDM signals

with moderate carrier-to-bandwidth ratios, where amplitude mismatch mostly contributes towards interference power in adjacent channels.

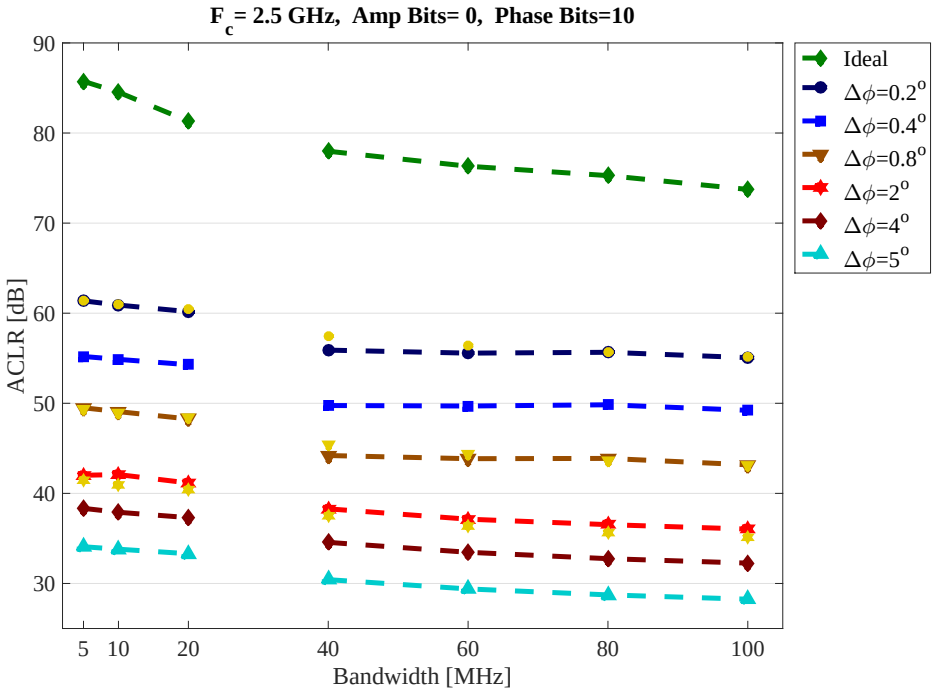

Figure 4.6: ACLR vs BW for (linear PA) LINC under phase imbalances, the theoretical values (yellow dots) are evaluated for 0.2, 0.8, and 2^o phase mismatches).

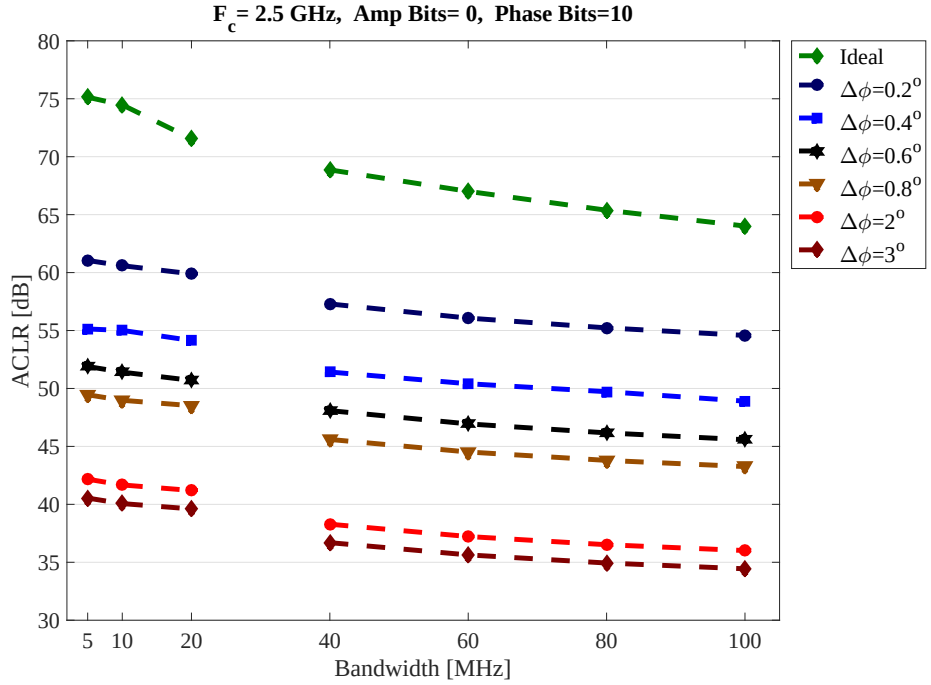

Figure 4.7: ACLR vs BW for (SMPA) LINC under phase imbalances.

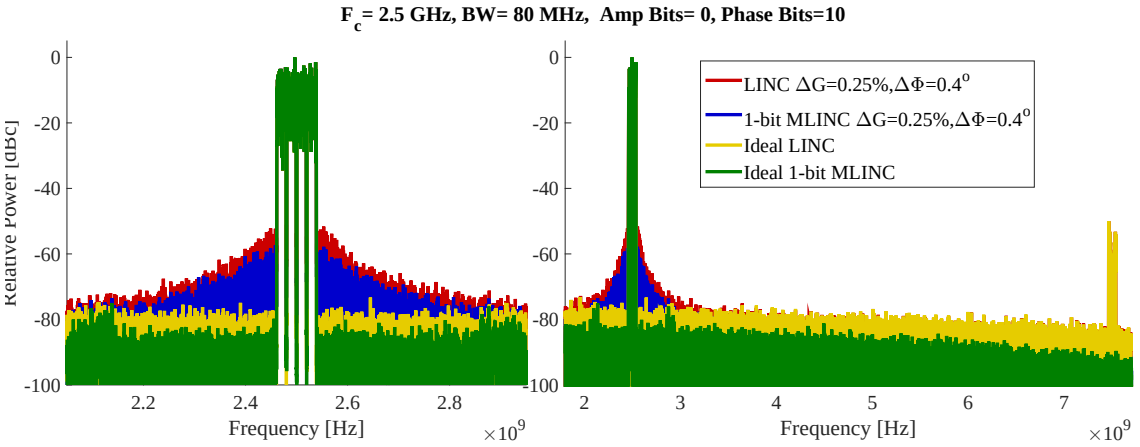

Figure 4.8: Spectra for LINC/MLINC schemes (Linear PA) under path mismatches: $\Delta G/G_o = 0.25\%$, $\Delta\Phi = 0.4^o$.

Fig. 4.6 and Fig. 4.7 illustrate ACLR results for the LINC transmitter (Linear PA and SMPA respectively) for the phase mismatch effects. The linearity performance of LINC (Linear PA) TX conforms with (3.4), the theoretical results are represented by yellow-colored symbols, suggesting that OOB distortion mainly arises from the uncanceled power quadrature signal during recombination. Linearity of the LINC schemes (Linear PA and SMPA) follows the same trends, under the influence of phase mismatches, as the performance of LINC TX for amplitude mismatch effects. Amplitude and phase mismatch originate from the same circuit imperfections, their impact on linearity performance of LINC transmitter is identical.

In order to meet the LTE downlink ACLR specification of 45 dB, amplitude imbalance of 1% and phase imbalance of 0.6^o (for both Linear PA and SMPA cases) is the maximum acceptable mismatch between LINC branches, given that all other performance parameters are ideal. This tolerance margin is further limited in practical transmitters, when other non-linearity inducing effects come into play.

4.3.2 MLINC Transmitter

Figure 4.8 illustrates the spectra of (Linear PA) LINC and MLINC schemes under the effects of path mismatches. ACLR of the ideal LINC TX for an 80 MHz OFDM signal is ~76 dB. It improves to ~81 dB for the ideal 1-bit MLINC TX, as the adjacent channel distortion, mostly contributed by quantization noise power, decreases with increase in amplitude resolution. Path mismatch (amplitude mismatch of 0.25% and phase mismatch of 0.4^o) reduces ACLR to ~50 dB and ~56 dB for LINC and MLINC schemes, respectively. These results show that linearity of outphasing transmitter, with and without path mismatches, improves by $5 - 6$ dB for 1-bit increase in amplitude resolution.

Figures 4.9 and 4.10 show linearity performance of 1-bit MLINC transmitter for

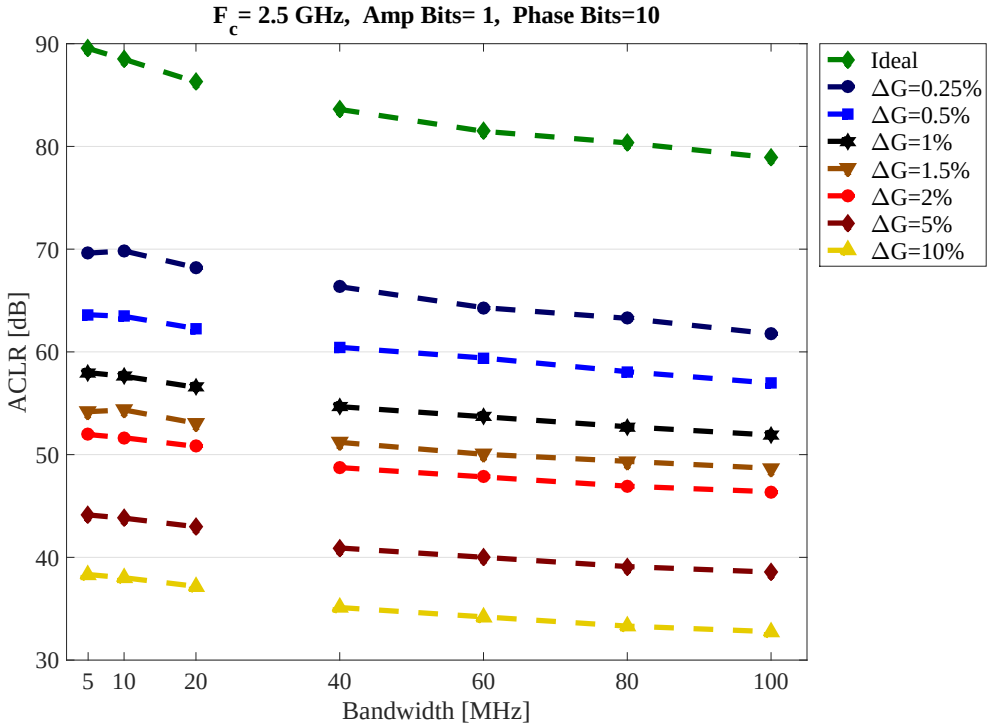

Figure 4.9: ACLR vs BW for (Linear PA) MLINC under amplitude imbalances.

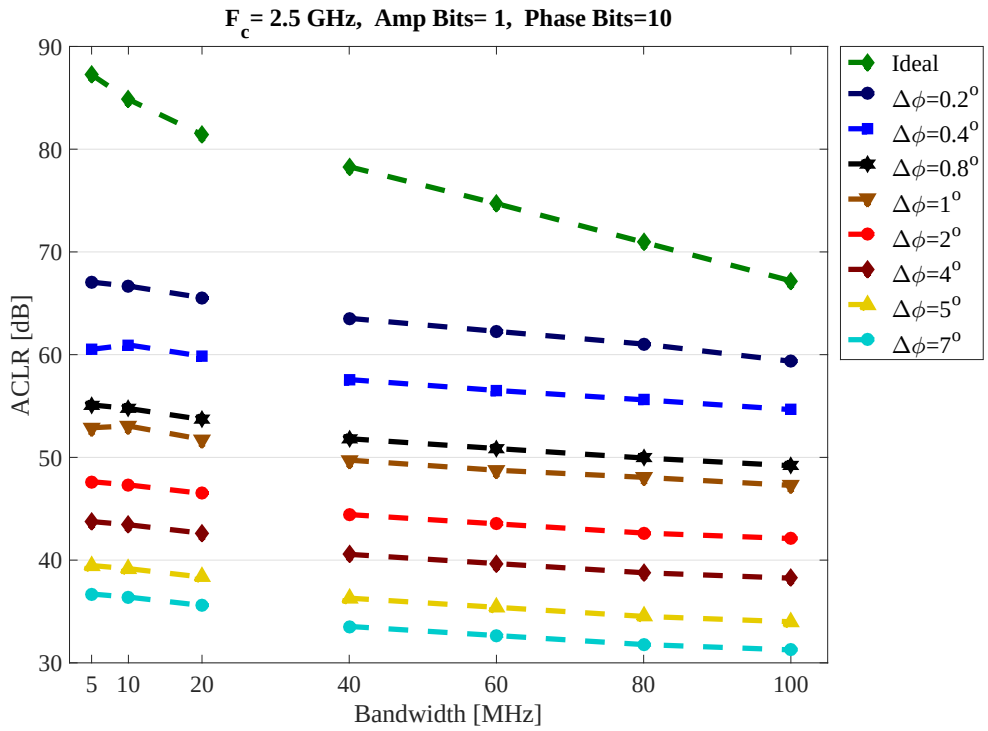

Figure 4.10: ACLR vs BW for (Linear PA) MLINC under phase imbalances.

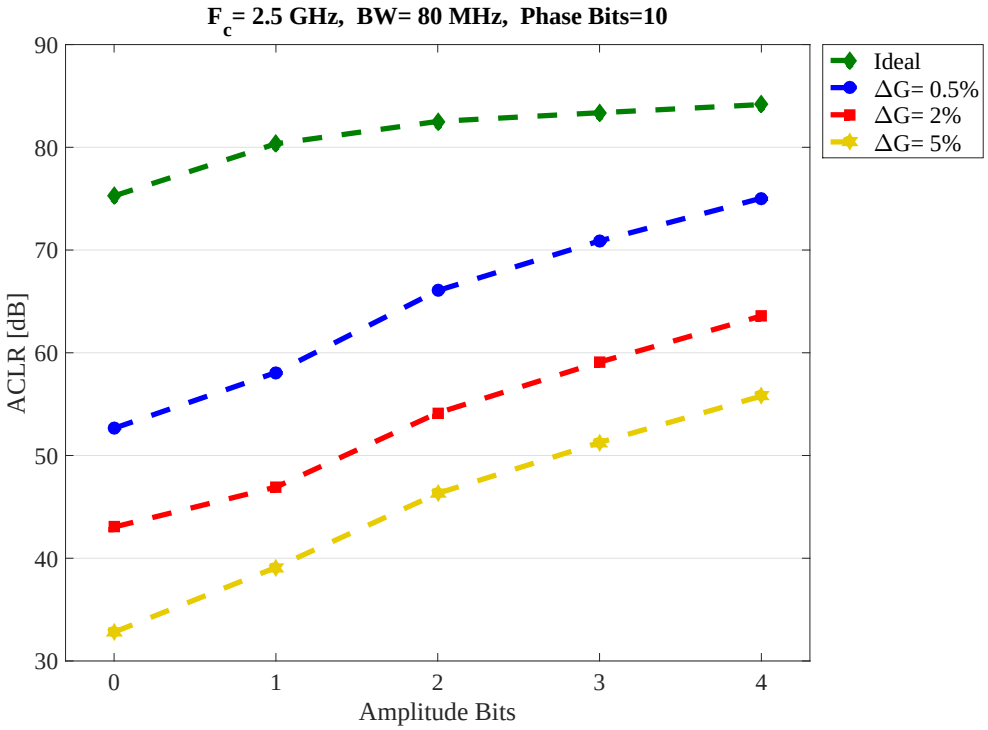

Figure 4.11: Multi-bit OT linearity performance under amplitude imbalances.

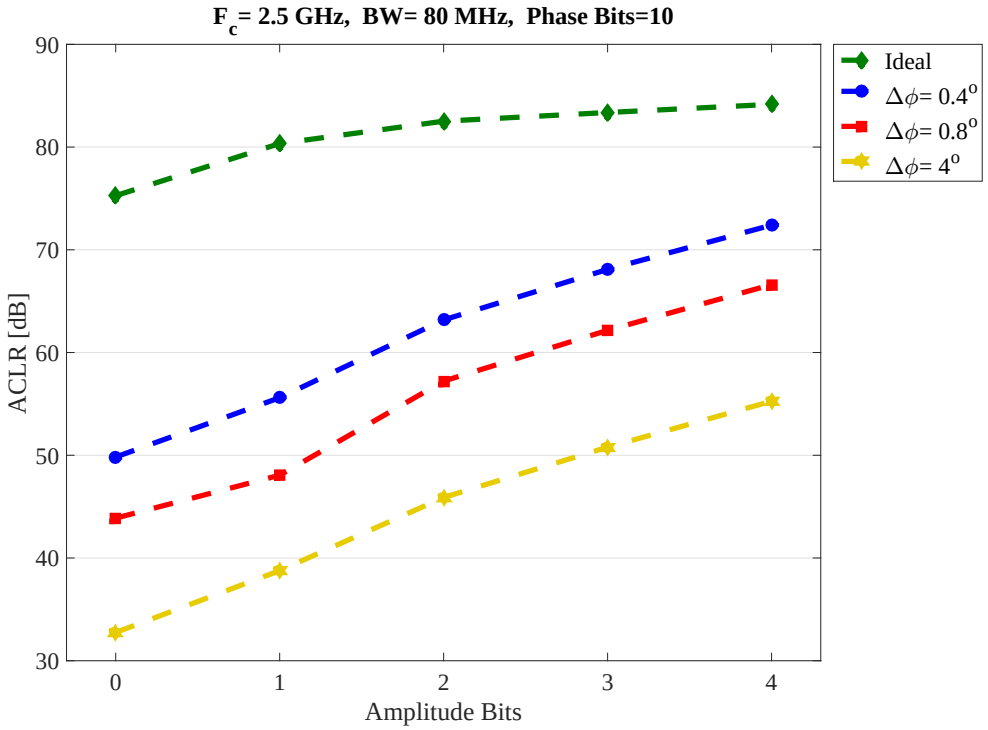

Figure 4.12: Multi-bit OT linearity performance under phase imbalances.

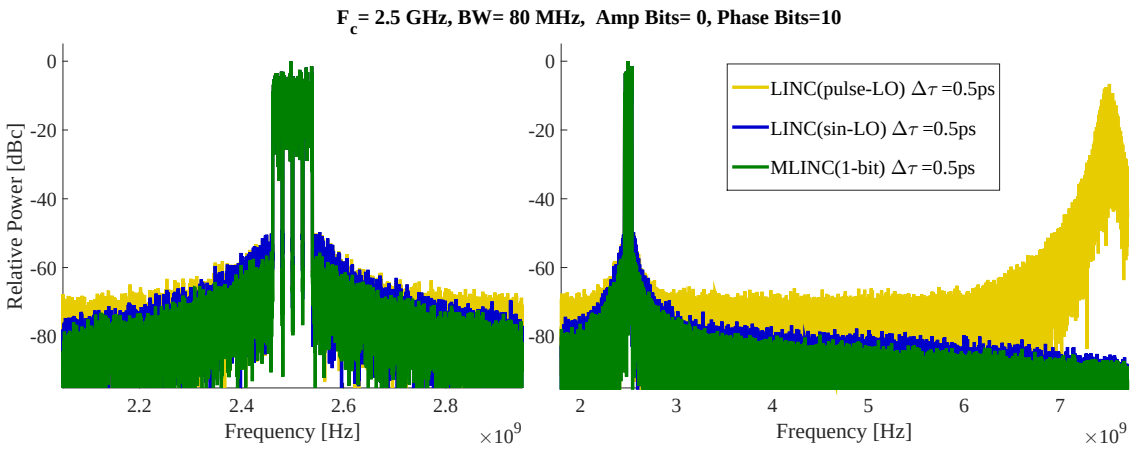

Figure 4.13: Outphasing Tx spectra for delay imbalance: $\Delta\tau = 0.5ps$.

multiple amplitude and phase mismatch cases. In comparison to the LINC scheme, ACLR for a particular amplitude/phase mismatch case improves by $3-7$ dB for 1-bit (2 amplitude levels) MLINC transmitter. OOB distortion in OT decreases with increase in amplitude bits, because the power of the quadrature signal, from (2.2), decreases with reduction in peak amplitude level α_{max}. In essence, in order to meet the LTE downlink ACLR specification of 45 dB, amplitude imbalance of 2%, and phase imbalance of 1^o is the maximum acceptable mismatch for (Linear PA) MLINC scheme, given that all other performance parameters are ideal. This tolerance margin will further shrink in practical transmitters as other non-linear effects come into play.

Fig. 4.11 and Fig. 4.12 demonstrate the attainable ACLR versus the number of amplitude bits of (Linear PA) outphasing transmitter under amplitude and phase imbalances, respectively. The results are obtained for 0-4 amplitude bit (1-16 amplitude levels) OT, under the effect of uniform path mismatch applied to each PA pair. The input signal is a 64-QAM OFDM signal of 80 MHz bandwidth and 10 bit phase resolution. ACLR of the outphasing transmitter improves around $5-9$ dB for increase in each amplitude bit (for all path mismatch cases). Thus, ACLR above a certain threshold can be maintained efficiently for higher amplitude bit outphasing transmitters. The tolerance margin for path mismatch effects improves with amplitude bit resolution, given that other nonlinearity inducing effects are negligible.

4.4 Delay Imbalance

In this section, linearity performance of outphasing transmitter is presented under delay mismatches. Propagation delay mismatch between the RF signals is created by inevitable process and component variations, it can considerably affect the linearity of outphasing transmitters. The ACLR results, illustrated in the following figures,

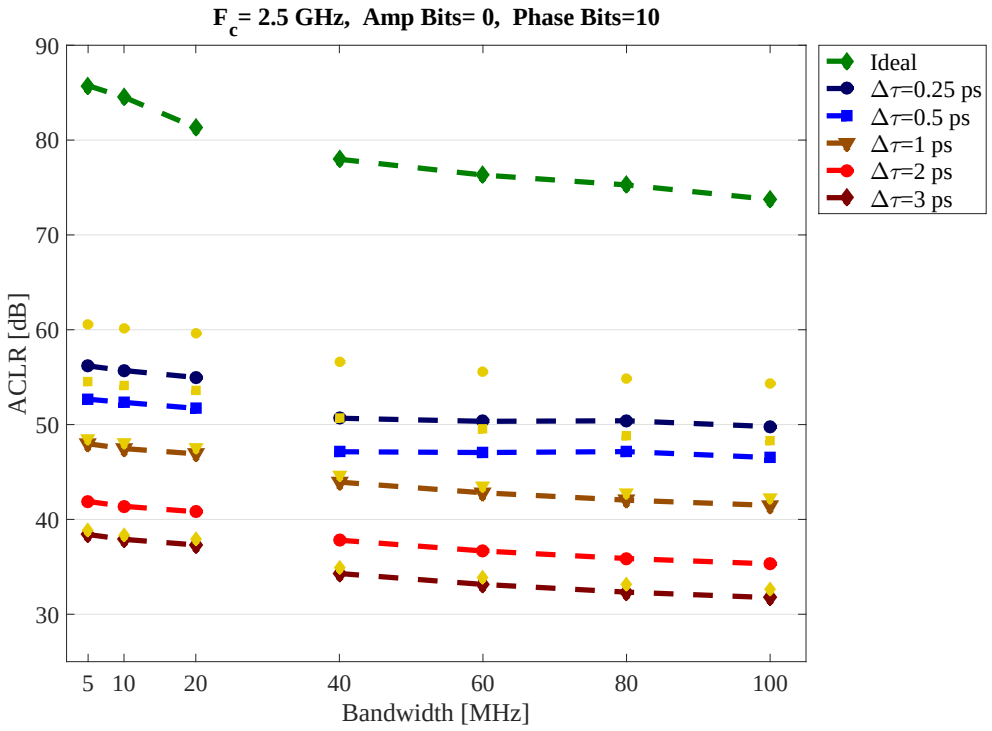

Figure 4.14: ACLR vs BW for (Linear PA) LINC under delay imbalances, the theoretical results (yellow dots) are evaluated for 0.25, 0.5, 1 and 3 ps delay mismatches.

are acquired for an ideal outphasing transmitter under the influence of a fixed delay mismatch, which is introduced to one of the RF branch signals.

Figure 4.13 illustrates the output spectra of LINC and MLINC schemes, under the influence of delay mismatch, $\Delta\tau = 0.5$ps. ACLR for LINC (Linear PA and SMPA) schemes is about 48 dB, which is mostly contributed by residual power of the quadrature signal $e(t)$ around the carrier frequency. The OOB distortion reduces in MLINC scheme due to higher amplitude bit resolution, and it exhibits ~6 dB improvement in ACLR for the same amount of delay mismatch present between RF signals.

4.4.1 LINC Transmitter

In Fig. 4.14, delay mismatch is varied between 0.25 to 3 ps for LINC (Linear PA) scheme. The results are acquired for a 64-QAM OFDM signal of 10 bit phase resolution. The linearity performance curves indicate that a delay mismatch of 0.25 ps can degrade ACLR of LINC TX by ~25 dB. Theoretical results obtained from (3.8), represented by yellow-colored symbols, vary from the simulated results. The difference probably arises from the approximation in (3.7). Since a phase mismatch approximation only grasps some of the effects of the delay mismatch, the theoretical results are giving optimistic values for the ACLR.

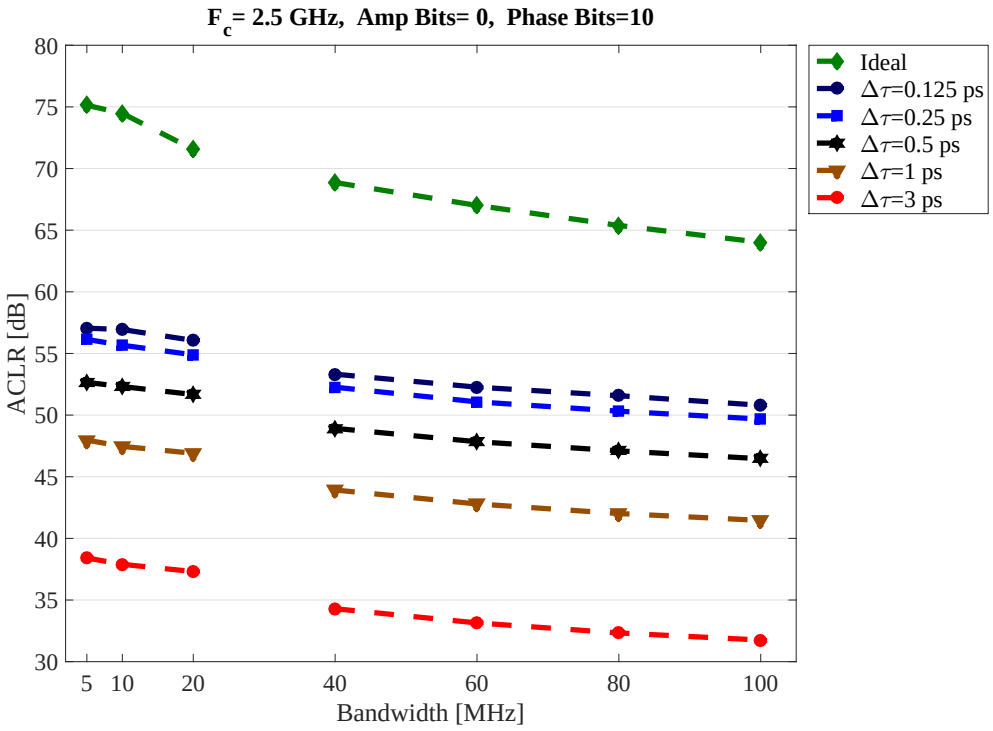

Figure 4.15: ACLR vs. BW for various delay mismatches for LINC (SMPA).

Figure 4.15 presents ACLR results for LINC (SMPA) scheme under delay imbalance range: 0.125 to 3 ps. The linearity performance results for this scheme are comparable to the results acquired for LINC (Linear PA) TX, suggesting that the residual power of the quadrature signal considerably influences OOB distortion for this case as well. As mentioned in section 4.1, these graphs represent performance of OFDM signals with moderate carrier-to-bandwidth ratios, where delay mismatch mostly contributes towards interference power in adjacent channels.

LTE downlink performance specifications can be satisfied for delay imbalance of $0.5ps$ for LINC (Linear PA and SMPA) TX, given that all other linearity influencing effects are negligible. The tolerance window in the range of picoseconds leads to stringent matching requirements for OT, this margin is further limited by other co-existing non-linearity inducing effects.

4.4.2 MLINC Transmitter

Figure 4.16 shows linearity performance of 1-bit MLINC transmitter under delay imbalance varied between 0.25 to 7 ps. In comparison to the LINC TX, ACLR for a particular delay mismatch case improves by $5-6$ for 1-bit (2 amplitude levels) MLINC transmitter. OT performance under delay mismatch follows similar trends as OT performance for path mismatch effects. A uniform (across each PA pair) delay mismatch of 1 ps is the maximum acceptable mismatch for a 1-bit MLINC

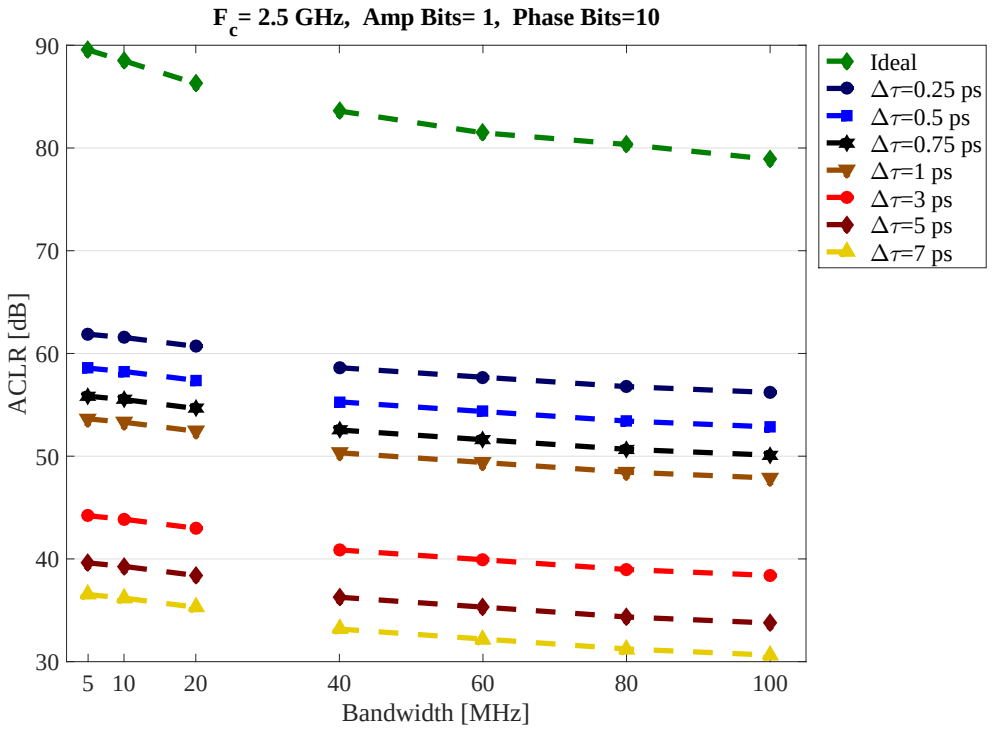

Figure 4.16: ACLR vs. BW various delay mismatches b/w MLINC branches.

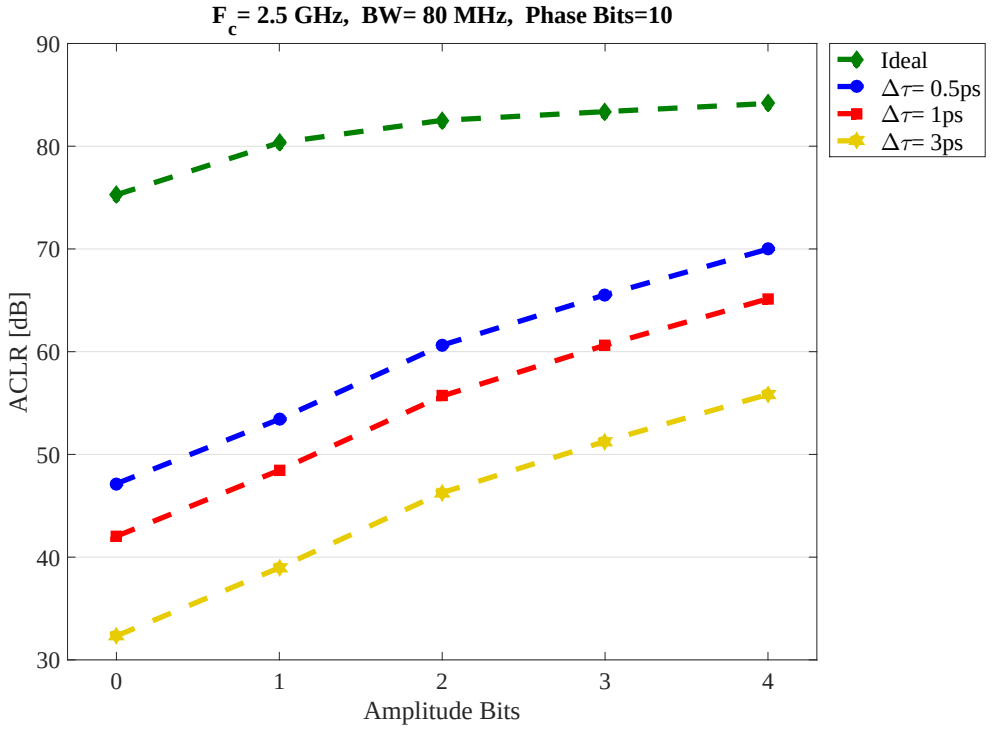

Figure 4.17: ACLR vs. amplitude bits for various delay mismatches between MLINC branches.

TX, given that other non-linear effects are negligible.

Fig. 4.17 demonstrates the achievable ACLR versus the number of amplitude bits of (Linear PA) outphasing transmitter under delay imbalances. The results are obtained for 0-4 amplitude bit (1-16 amplitude levels) OT, under the effect of uniform path mismatch applied to each PA pair. The input signal is a 64-QAM OFDM signal of 80 MHz bandwidth and 10 bit phase resolution. ACLR of the outphasing transmitter improves around $5-7$ dB for increase in each amplitude bit (for all delay mismatch cases). ACLR above a certain threshold can be maintained efficiently for higher amplitude bit outphasing transmitters. The tolerance margin for delay mismatch effects also improves with amplitude bit resolution, given that other nonlinearity inducing effects are negligible.

4.5 Quadrature Modulator Mismatches

This section analyzes the effects of IQ modulator errors on the outphasing transmitter. I and Q components of outphased signals experience different gains and phase shifts in I- and Q- branches respectively. In addition, a portion of the unmodulated RF carrier appears in the modulator branch paths due to the LO leakage effect. IQ mismatches cause the PM signals to have a non-constant envelope, which could lead to AM/AM and AM/PM distortion in the PAs. IQ modulator imbalances also result in partial cancellation of the quadrature signal during recombination. I/Q modulator impairments are usually described in terms of differential gain g_d, differential phase Φ_d and carrier leakage c, as was described in Section 3.3. Outphasing transmitter utilizes at least two phase modulators, and naturally each branch signal experiences a unique set of parameters.

Outphasing transmitter is built around the idea that a major portion of nonlinearity generated by the power amplifier can be avoided for constant envelope signals. But spurious amplitude modulation is inevitable in practical transceivers and it creates distortion. I/Q modulator errors are one of the contributing factors to amplitude variation in pure phase modulated signals. The results presented in this section are obtained for scenarios built to understand the two-fold effect of I/Q errors: residual power of quadrature signal at the combiner output and inter-modulation distortion created by PA non-linearity. The quadrature modulator impairments are simulated for the following scenarios:

- Scenario A: I/Q modulators function in an ideal manner i.e. without any imbalances or imperfections.

- Scenario B: It generates a small I/Q error with slight variation in the parameter values of both branches. The I/Q error parameters utilized here are as follows: $g_d = 0.05$ dB, $\Phi_d = 0.05^o$ for phase modulator of branch 1 and $g_d = 0.03$ dB,

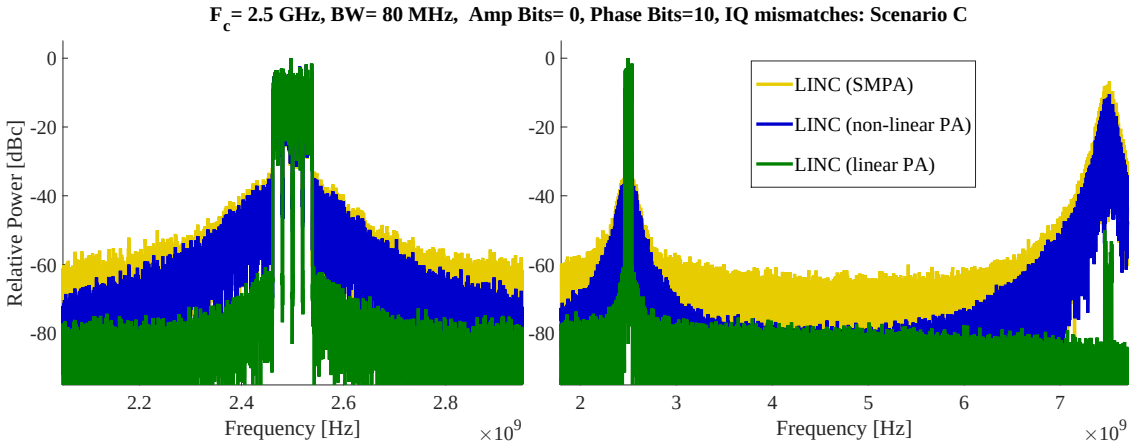

Figure 4.18: Outphasing Tx spectra under IQ modulator mismatches: Scenario D.

$\Phi_d = 0.03^o$ for phase modulator of branch 2 with carrier leakage -63 dBc (in both modulators). These impairments create amplitude modulation in the up-converted signals, the range of envelope variation, obtained from (3.10), is $\pm 0.36\%$ and $\pm 0.245\%$ of input signal magnitude α_{max}, in branches 1 and 2 respectively [30].

- Scenario C: I/Q modulator parameters used for this scenario are: $g_d = 0.1$ dB, $\Phi_d = 0.1^o$ for phase modulator of branch 1 and $g_d = 0.14$ dB, $\Phi_d = 0.14^o$ for phase modulator of branch 2 with carrier leakage -63 dBc (in both modulators). These errors leads to amplitude variation in the modulated signals, the range of envelope variation is $\pm 0.656\%$, and $\pm 0.89\%$ of α_{max}, in branches 1 and 2 respectively.

- Scenario D: I/Q modulator parameters used in this scenario are as follows: $g_d = 0.7$ dB, $\Phi_d = 0.7^o$ in phase modulator of branch 1 and $g_d = 0.74$ dB, $\Phi_d = 0.74^o$ in phase modulator of branch 2 with carrier leakage -61.9 dBc (in both modulators). These resultant amplitude variation is $\pm 4.3\%$ and $\pm 4.56\%$ of α_{max}, in branches 1 and 2 respectively.

- Scenario E: I/Q modulator parameters used in this scenario are as follows: $g_d = 1$ dB, $\Phi_d = 1^o$ in phase modulator of branch 1 and $g_d = 1.2$ dB, $\Phi_d = 1.2^o$ in phase modulator of branch 2 with carrier leakage -61.9 dBc (in both modulators). These resultant amplitude variation is $\pm 6.24\%$ and $\pm 7.56\%$ of α_{max}, in branches 1 and 2 respectively.

Figure 4.18 illustrates the spectra of outphasing transmitter with linear, non-linear and switch-mode PAs under the influence of IQ modulator mismatches (Scenario D). Outphasing transmitter (Linear PA) achieves an ACLR of ~59 dB under IQ errors, which is largely constrained by the residual power of $e(t)$. PA non-linear

effects combined with IQ errors reduce ACLR to 33.1 dB and 31 dB for non-linear and switch-mode PA cases, respectively. The envelope fluctuation in the non-linear and switch-mode power amplifiers results in a significant amount of intermodulation distortion in the outphasing transmitters.

In Fig. 4.19, Fig. 4.20 and Fig. 4.21, ACLR results are illustrated for linear, non-linear and switch-mode PAs respectively, under the influence of quadrature modulator mismatches. IQ modulator mismatches create amplitude and phase distortion in the RF phased modulated signals, which leads to linearity degradation in outphasing transmitters. The best ACLR results for the given IQ mismatches are obtained for (Class A) OT, and lowest ACLR results are achieved for (SMPA) OT. Because, Linear PAs do not induce any non-linearity in OT, the residual power of the quadrature signal chiefly contributes towards OOB distortion. The IQ errors create intermodulation distortion in (non-linear PA) OT due to AM-AM and AM-PM conversion effects, which reduces the ACLR by $9-16$ dB (in comparison to Linear-PA OT). The IQ mismatches also create intermodulation distortion in (SMPA) OT, which degrades ACLR by $10-17$ dB (in comparison to Linear-PA OT), for the simulated IQ modulator imbalances.

In order to meet the LTE downlink ACLR specification of 45 dB, IQ modulator mismatches presented in Scenario C are the maximum acceptable mismatches for non-linear PA and SMPA outphasing transmitters, given that all other performance parameters are ideal. This tolerance margin is further limited in practical

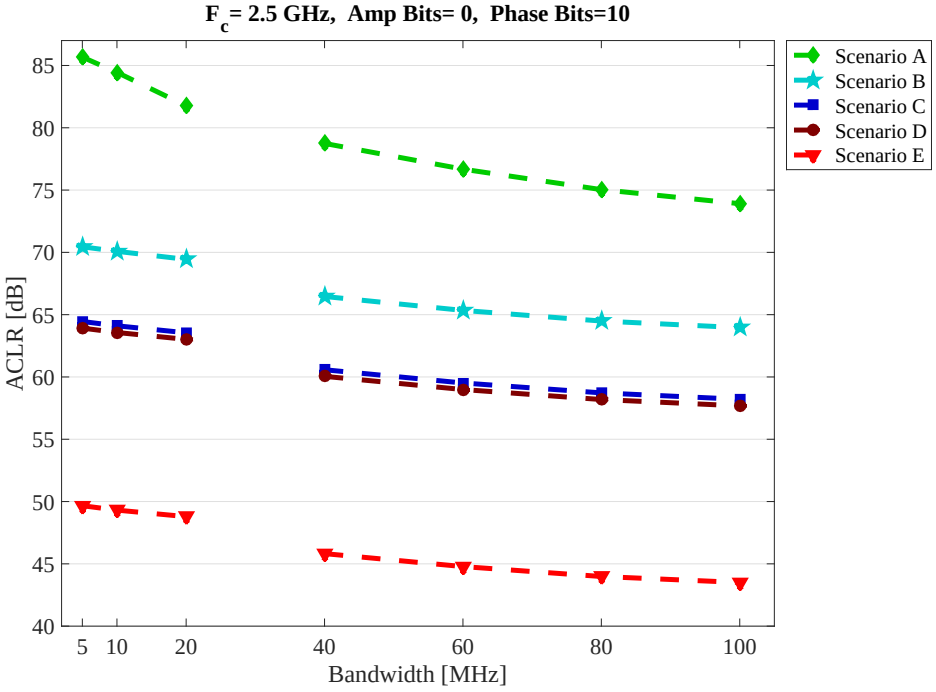

Figure 4.19: ACLR vs BW for (linear PA) OT under I/Q modulator errors.

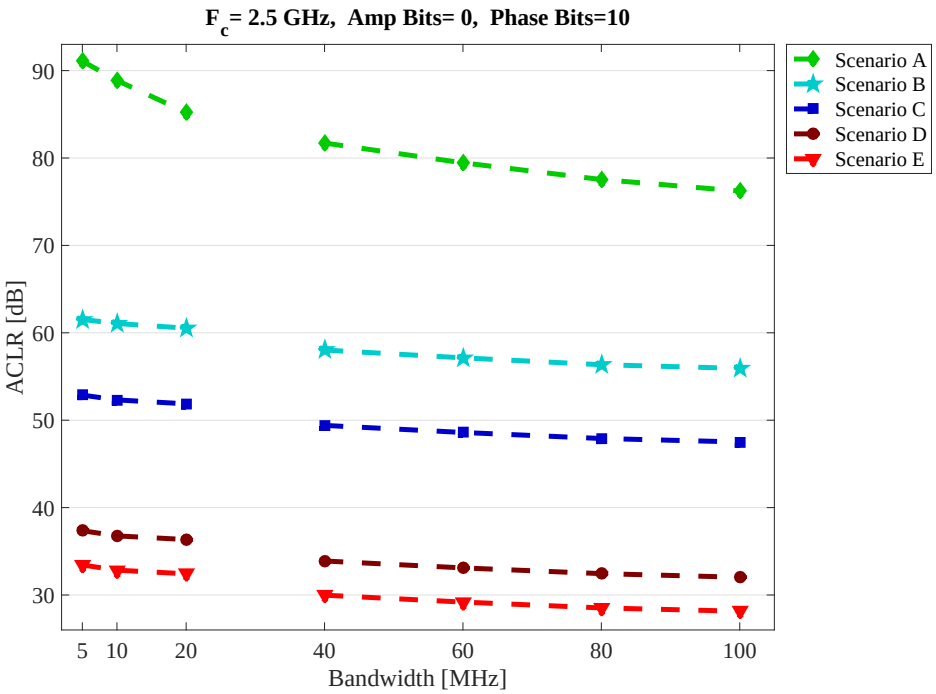

Figure 4.20: ACLR vs BW for (non-linear PA) OT under I/Q modulator errors.

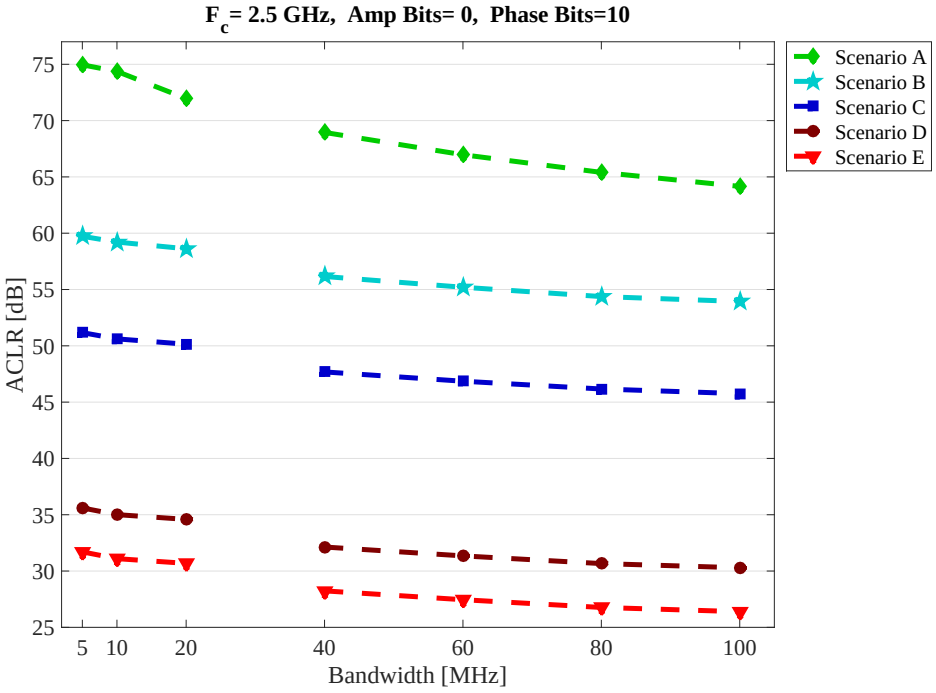

Figure 4.21: ACLR vs BW for (SMPA) OT under I/Q modulator errors.

transmitters in the presence of other non-linear effects.

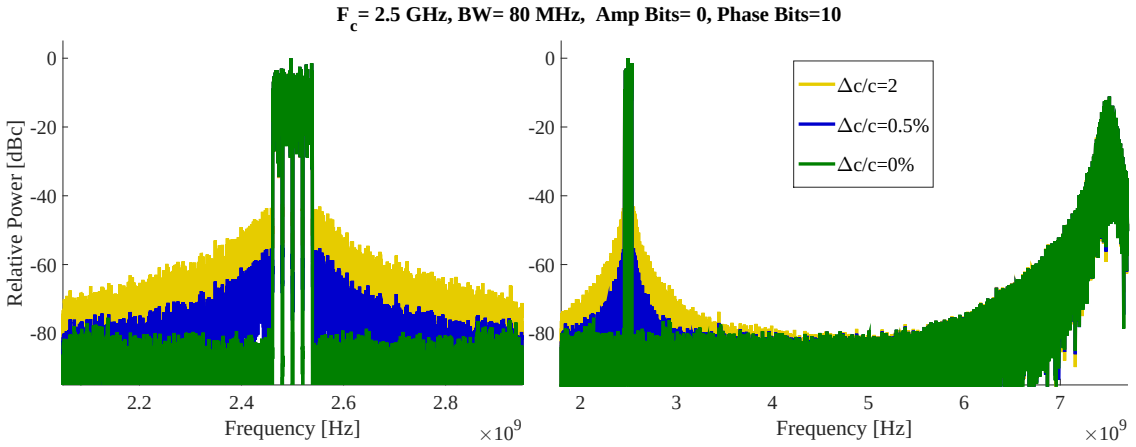

Figure 4.22: Outphasing transmitter spectra for variation in the third-order characteristics ($\Delta c/c$) of non-linear PAs.

4.6 PA Imperfections

This section discusses the differences in non-linear characteristics of power amplifiers and their impact on the linearity of the outphasing transmitters.

4.6.1 PA non-linear characteristics

Due to process and component tolerances, power amplifiers in symmetric RF paths

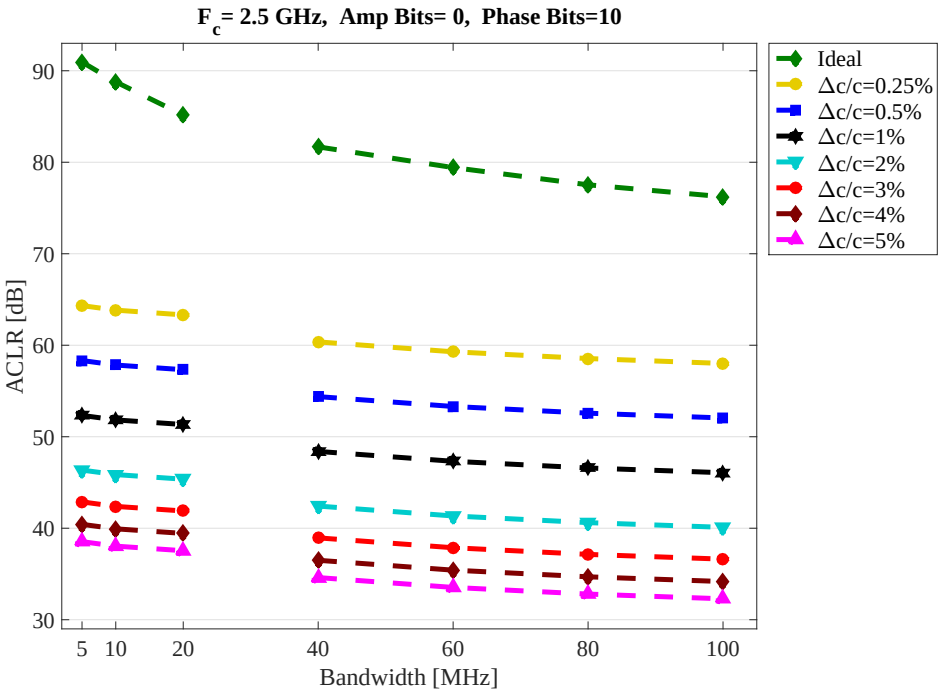

Figure 4.23: ACLR vs BW of (non-linear PA) OT for for variation in the third-order characteristics ($\Delta c/c$).

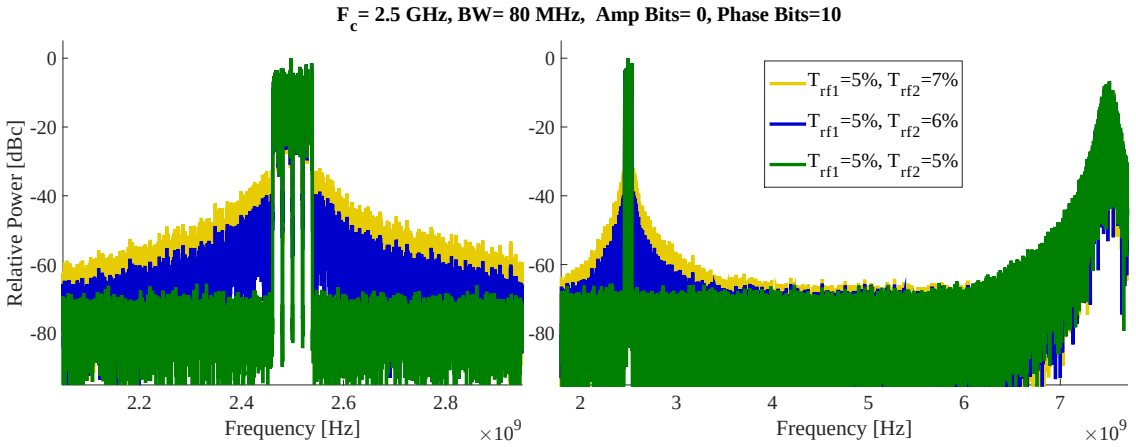

Figure 4.24: Outphasing transmitter spectra under finite rise/fall time.

are not matched; PAs exhibit dissimilar non-linear characteristics, which affects the linearity performance of outphasing transmitters. Figure 4.22 illustrates the spectra of (non-linear PA) LINC scheme under the effects of dissimilar PA third-order characteristics (Δc). The achieved ACLR for a balanced OT with identical PAs is about 78 dB, which reduces to 53 dB and 41 dB for the mismatches (0.5% and 2% $\Delta c/c$, respectively) in third-order characteristics of the PAs.

Figure 4.23 shows the ACLR results for outphasing transmitters under the influence of mismatches in PA third-order characteristics (Δc). PA nonlinearity with ideal phase modulated signals induces interference only if the PA nonlinear responses are different, in which case the effect is equivalent to a gain mismatch. The LTE downlink specifications can be met for an outphasing transmitter with 1% variation in the third-order characteristics of the branch power amplifiers. This tolerance window will further be limited in practical power amplifiers, exhibiting higher-order non-linearity and memory effects.

4.6.2 Finite Rise/Fall Time

The realistic pulses of SMPA driving signals are trapezoidal in nature, these pulses affect the efficiency and linearity of the outphasing transmitters. Figure 4.24 shows the spectra of the outphasing transmitter for pulsed signals with finite rise- and fall-time. The outphasing transmitter, with uniform rise/fall time in both branches, does not introduce any additional interference power, besides the interference created in square-wave carrier based OT due to the mixing of DAC images with the carrier harmonics. The mismatch in the pulse rise/fall time introduces distortion, resulting in ACLR of about 40 dB and 30 dB for 1% and 2% difference in rise/fall times (T_{rf}) of the RF signals, respectively.

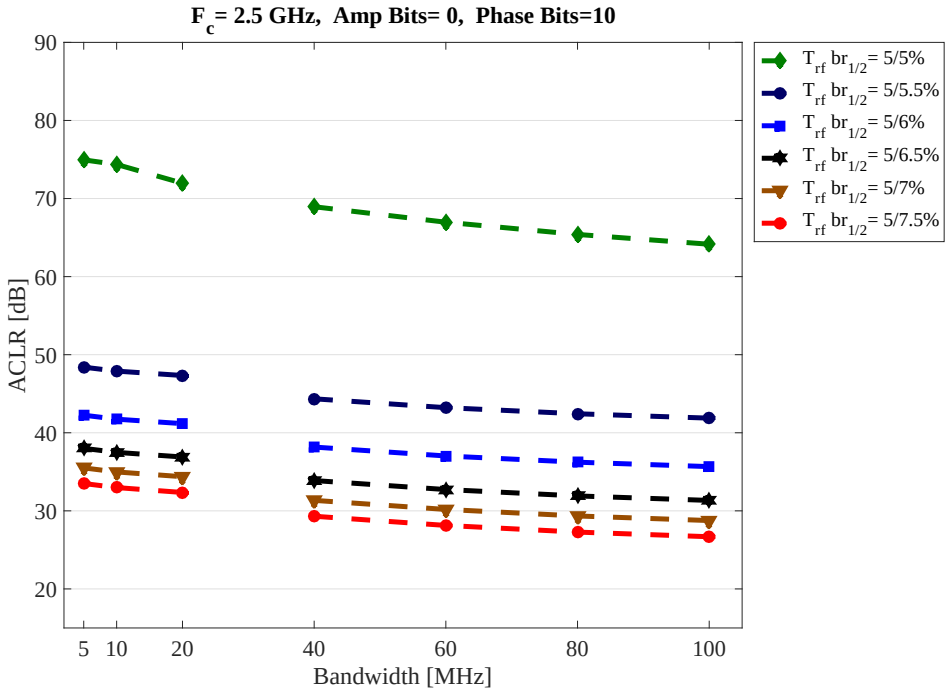

Figure 4.25: ACLR vs BW for (SMPA) OT exhibiting finite rise/fall time.

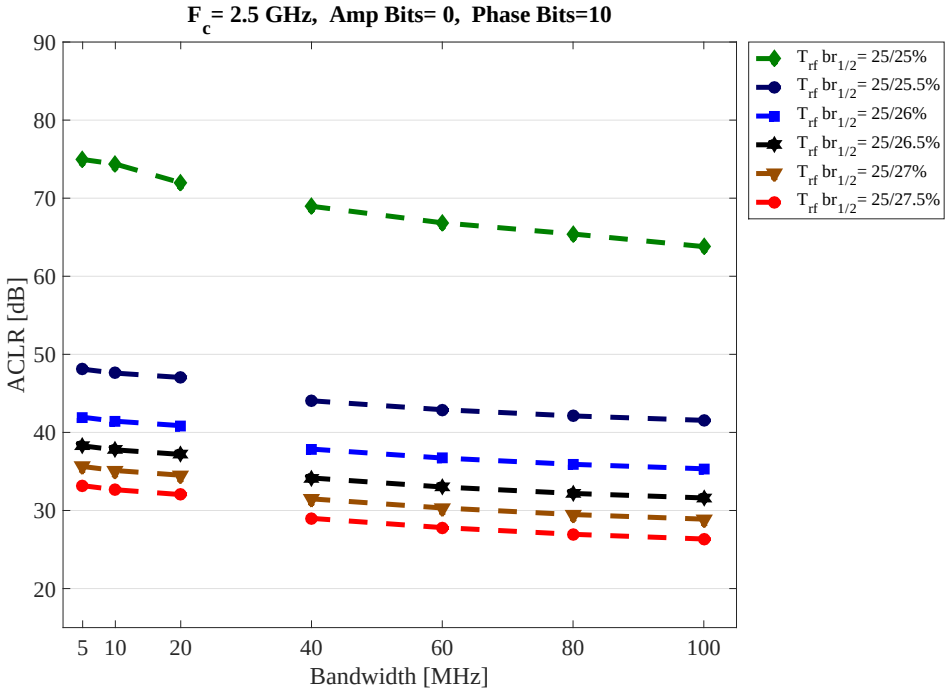

Figure 4.26: ACLR vs BW for (SMPA) OT exhibiting finite rise/fall time.

Figure 4.25 shows the linearity performance of (SMPA) LINC transmitter under the effects of finite rise- and fall- time. The ACLR results for uniform rise/fall time of 5% in both branch signals, are comparable to the ACLR results acquired for an

ideal/balanced (SMPA) LINC TX (see Scenario A in Fig. 4.21). ACLR degrades with the increase in mismatch of rise/fall time between the branch signals.

The linearity performance of the outphasing transmitter is not much affected (up to a certain limit) by the absolute rise/fall time, this is demonstrated with the help of Fig. 4.26. The ACLR results under a uniform rise/fall time of 25% (of the pulse time period) are similar to the ACLR results achieved for the uniform rise/fall time of 5% (of the pulse time period). Moreover, the ACLR results in Fig. 4.26 follow the same trends as the results shown in Fig. 4.25. Thus, the linearity of outphasing transmitters depends only on the relative mismatch (up to a certain limit) in rise- and fall- time of the outphasing branch signals. In order to meet LTE downlink specification of 45 dB ACLR, less than 0.5% difference in rise/fall time can be tolerated in the outphasing transmitters. This tolerance margin will further be limited in practical (SMPA) outphasing transmitters due to other co-existing non-linear effects.

4.7 Linearity of Chireix Outphasing TX

This section discusses the nonlinearity introduced by lossless combiners and its effect on the overall performance of the (ideal) outphasing transmitter. The performance results of 0-bit outphasing transmitter are presented for the hybrid and Chireix combiners.

Figure 4.27 shows the spectra of (SMPA) OT with the hybrid and Chireix combiners. ACLR for an ideal transmitter i.e. balanced OT with a hybrid combiner is 65 dB. The Chireix combiner creates amplitude and phase distortion in the outphasing transmitter, and reduces the ACLR to ~29 dB and ~13 dB for the stub electric lengths of 1^o and 82^o, respectively. The stub electric length, for the later case, is evaluated for the most occurring signal level, which is 82^o for this realization.

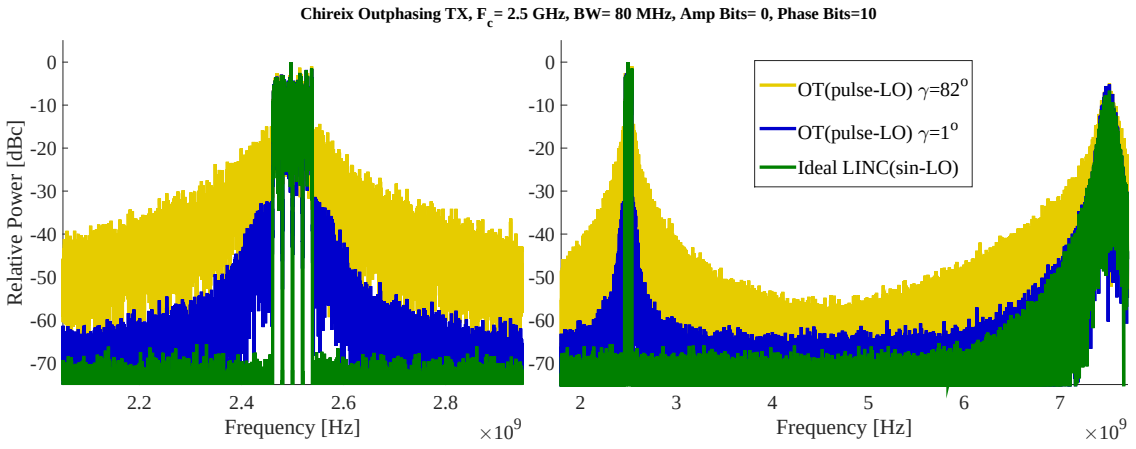

Figure 4.27: Outphasing transmitter spectra for Hybrid and Chireix combiners.

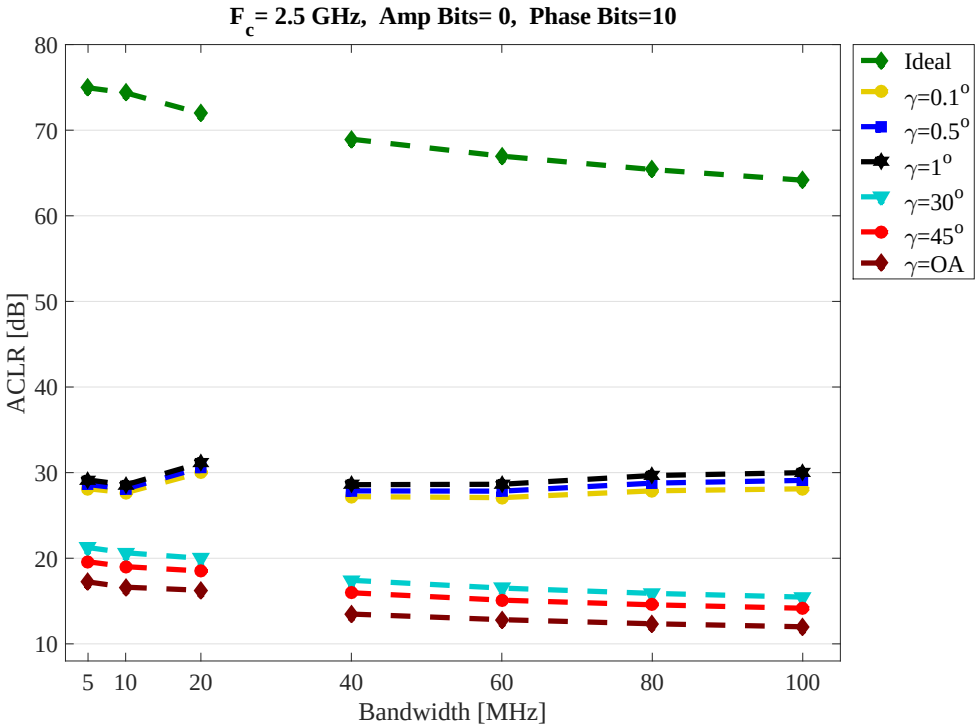

Figure 4.28: ACLR simulation results for Chireix OT with SMPA.

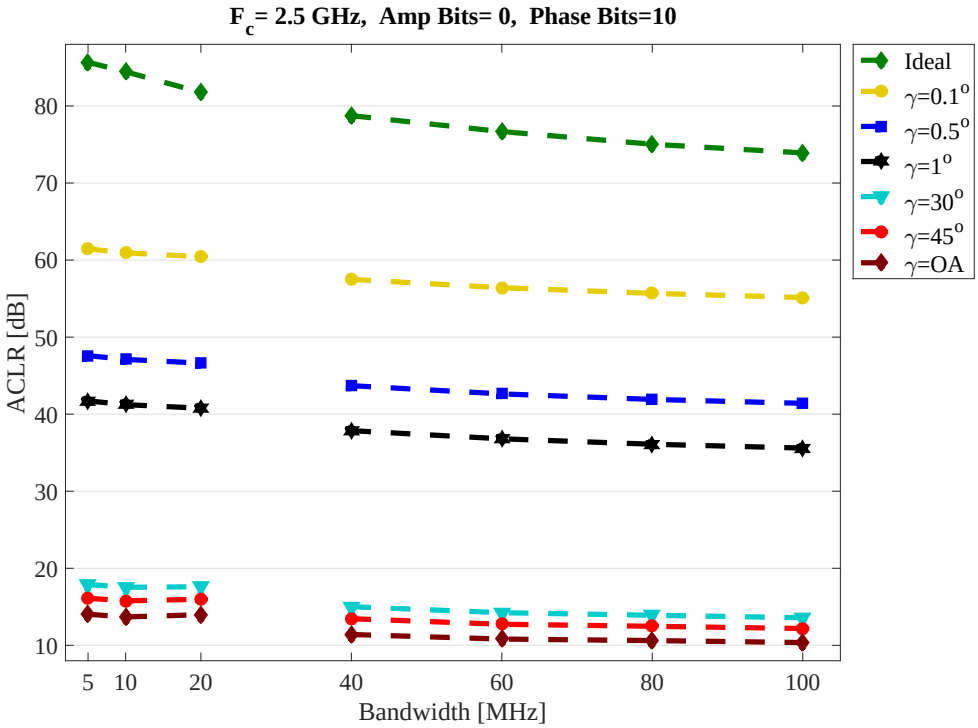

Figure 4.29: ACLR simulation results for Chireix OT with Linear PA.

Table 4.1: PAPR and most frequently occurring $\theta(t)$ of multicarrier OFDM signals.

BW (MHz)	5	10	20	40	60	80	100
PAPR (dB)	7.93	8.1	8.98	9.57	9.97	10.5	10.79
$\theta(t)$ (deg)	73.4	74.4	75.9	78.6	77.89	78.75	79.05

In Fig. 4.28 the Chireix (SMPA) outphasing TX results are presented for various stub electric lengths γ. The ACLR results are acquired for a 64-QAM OFDM signal of 0 bit amplitude and 10 bit phase resolution. The Chireix combiner parameters are evaluated for the specific stub electric lengths, following the design procedure adopted in [23]. The ideal ACLR curves (green-colored) represent the performance of OT with a hybrid combiner, which a linear combiner. The linearity performance of (SMPA) OT with the hybrid combiner is restricted only by the interference created by the mixing of DAC with the carrier harmonics, as discussed in Section 4.2. While, the Chireix combiner nonlinear effects create a significant amount of distortion in outphasing transmitters, and reduce the ACLR to $<$ 30 dB. The combiner nonlinearity creates a significant amount of distortion in the OOB region even for stub electric lengths varying between 0.1^o and 1^o. The multicarrier OFDM signals exhibit high PAPR, naturally the probability density function (PDF) for the outphasing angle $\theta(t)$ is uneven with high occurrence of angles close to 90^o. As shown in 4.1, the most frequently occurring outphasing angle is $> 70^o$ for all the simulated cases. The ACLR results of Chireix outphasing TX obtained for $\theta(t)$ between 30^o and 80^o are $<$ 20 dB. Hence, Chireix outphasing transmitters with SMPAs exhibit high efficiency at the cost of severe degradation of linearity.

Figure 4.29 shows linearity performance results of Chireix OT with linear power amplifiers. Though, this architecture is not feasible practically (as discussed in Sections 2.1 and 2.4.1), it is simulated for the purpose of examining the effect of stub length on the linearity of Chireix outphasing transmitters. Chireix combiners introduce a significant amount of distortion even in the linear/balanced outphasing transmitters, but the ACLR results are much worst for (SMPA) Chireix OT (indicating that carrier harmonics are mixing with Chireix combiner induced non-linearity). Both cases produce similar ACLR results for large outphasing angles. It can be observed that the linearity performance of OT depends on the stub's electric length γ, as was discussed in Section 3.5.

Chireix outphasing transmitters for SMPAs do not meet the LTE downlink ACLR specification of 45 dB for any simulated cases. The digital phase predistortion may be used to linearize Chireix transmitters [43], [44].

5. CONCLUSIONS

5.1 Research Summary

In this thesis, a quantitative analysis of the linearity performance of outphasing radio transmitters is presented for LTE base station applications, under RF path mismatches and non-linear effects. The major contributors towards linearity degradation in outphasing transmitters have been discussed, and their impact is analyzed in terms of ACLR specifications for LTE downlink transmission.

Theoretical analysis complemented by simulation results showed that path imbalance and delay imbalance are one of the major contributing factors to the ACLR degradation in outphasing transmitters. These mismatches result in only partial cancellation of the wideband quadrature signal at the combiner output. Quadrature signal power constitutes a considerable amount of interference in the LINC transmitter, diminishing the impact of quantization noise on the linearity of LINC transmitter.

IQ modulator mismatches, present within each phase modulator and between the branch phase modulators, introduce amplitude and phase modulation into the phase modulator output signals. The quadrature modulator mismatches, in conjunction with amplifier nonlinearity, result in a significant amount of spectral regrowth in the out-of-band region, as well as in-band interference. The amplitude modulation, created by quadrature mismatches, produces a large amount of intermodulation distortion in outphasing transmitter with switch-mode PAs.

Power amplifiers heavily influence linearity of outphasing transmitters. A small mismatch in non-linear characteristics of branch PAs results in significant distortion around the carrier frequency. Realistic square-wave signals exhibit finite rise- and fall- time, which also creates spectral leakage in the combined signal. Any amplitude modulation in the phase modulated signals (due to e.g. IQ modulator imbalance), will make PA nonlinearity effects much worse. The ACLR results for outphasing transmitters indicate that the relative values of mismatches (in symmetric RF paths) are more important for obtaining minimal distortion, than the absolute mismatches encountered in the respective branches.

In outphasing transmitters with hybrid combiners, non-linearity is either caused by the branch imbalances or PA non-linear effects. Chireix outphasing transmitters, on the other hand, create a significant amount of distortion in OOB region. It was

Table 5.1: Max. tolerable imbalances (to keep ACLR > 45 dB) in outphasing TX.

Imbalance	$\Delta G/G$	$\Delta\Phi$	$\Delta\tau$	IQ errors	$\Delta c/c$	ΔT_{rf}	Chireix OT
LPA-LINC	1%	0.6^o	0.5 ps	Scenario D [1]	1% [2]	-	-
SMPA-LINC	1%	0.6^o	0.5 ps	Scenario C [1]	-	$< 0.5\%$	stubless
1-bit MLINC[3]	2%	1^o	1 ps	-	-	-	-
2-bit MLINC[3]	$< 5\%$	$< 4^o$	< 3 ps	-	-	-	-

observed, that the Chireix combiner induced non-linearity is the dominant source of interference, because ACLR is low even with the linear PAs, but much worse with SMPAs (indicating that the carrier harmonics are mixing with Chireix combiner non-linearity). The ACLR results also highlight that electrically longer stubs are more non-linear, which is unfavorable for OFDM signals (largely exhibiting outphasing angles close to 90^o, thus requiring longer stub lengths). This makes mandatory the compensation of Chireix combiner induced non-linearity in outphasing transmitters.

Table 5.1 represents the maximum tolerable mismatches, in outphasing transmitters,for LTE downlink ACLR specification of 45 dB. Such accuracy is impractical in real implementations, and therefore some form of linearization is needed in outphasing transmitters. The tolerance margin for each mismatch will further be limited in practical circuits, when all these non-linearity inducing effects co-exist in outphasing transmitters.

5.2 Future Research Directions

The linearity of outphasing transmitters is a broad research topic, which includes the discussion of distortion created in the in-band and out-of-band frequency regions. The system-level model could be built to analyze in-band distortion through error vector magnitude (EVM). Furthermore, the model can be developed to include specific models such as PA models, in order to accurately predict the linearity of outphasing transmitters, and analyze their performance for various compensation/linearization techniques. Multi-level outphasing transmitter performance can be analyzed under non-uniform mismatches and the simulation results can be authenticated by the prototypes of outphasing transmitter.

[1] See Section 4.5
[2] Results for non-linear PAs characterized by Ghorbani model
[3] For Class A (LPA)

A. APPENDIX A

A.1 Input signal expressions of Chireix combiner

This appendix presents the output expressions for the PAs and the Chireix combiner resulting from the reflection effects, caused by impedance mismatch between the amplifiers and the combiner. The PA output expressions were utilized in the Matlab simulator to analyze the linearity performance of the Chireix outphasing transmitter.

Considering a Chireix outphasing transmitter shown in Fig. 3.6 (presented in Section 3.5). The RF power amplifiers are assumed to be identical i.e. having a real voltage gain G and an output impedance of Z_o. The Chireix combiner consists of the following: transmission lines having impedance Z_c, two stubs of susceptance B and a tee junction. The input ports of the Chireix combiner are not matched to the output ports of RF PAs, resulting in reflections. The reflected signals add with the incoming signal and modify the existing outphasing angle $\theta(t)$ to $\theta'(t)$. From [37], the branch signals are composed of incident and reflected signals, expressed as

$$\begin{aligned} S_{PA,1}(t) &= \alpha_o G\big|1+\Gamma(\beta,\theta'(t))\big|cos\big(w_c t+\phi(t)+\theta'(t)\big) \\ S_{PA,2}(t) &= \alpha_o G\big|1+\Gamma(-\beta,-\theta'(t))\big|cos\big(w_c t+\phi(t)-\theta'(t)\big), \end{aligned} \tag{A.1}$$

where, $\Gamma(-\beta,-\theta'(t))$ and $\Gamma^*(\beta,\theta'(t))$ are the reflection coefficients seen by the power amplifiers. These reflection coefficients depend on the stub constant β, which is expressed as

$$\beta = \frac{B{Z_c}^2}{Z_L},$$

and the modified outphasing angle $\theta'(t)$. Here, Z_L is the load impedance of the Chireix combiner. The reflection coefficients for the two power amplifiers are equal,

$$\Gamma(-\beta,-\theta'(t)) = \Gamma^*(\beta,\theta'(t)),$$

which follows that the PA output signals have the same magnitude and opposite phases as a function of time [37]. $S_{PA,1}(t)$ and $S_{PA,2}(t)$ are summed in the combiner to obtain,

$$S_{OUT} = S_{PA,1}(t)+S_{PA,2}(t) = 2y\alpha_o G\big|1+\Gamma(\beta,\theta'(t))\big|cos\big(w_c t+\phi(t)\big)cos(\theta'(t)), \tag{A.2}$$

here, $y = (Z_o/Z_c)$ is the normalized characteristic admittance of the Chireix lines. The combiner output in A.2 is expressed in terms of the modified outphasing angle $\theta'(t)$. From [23], it can also be expressed as a function of the $\theta(t)$

$$S_{OUT}(t) = \frac{2y\alpha_o G cos\gamma}{1 + 2y^2 cos^2\gamma} cos\big(w_c t + \phi(t)\big) cos\big(\theta(t) - \gamma\big), \tag{A.3}$$

where, γ is the electrical stub length and $\gamma = tan(y^2\beta)$. In order to express power amplifier output signals in terms of the original outphasing angle, the following derivation is undertaken. From A.1 and A.2, we can observe that

$$S_{PA,1/2}(t) = \frac{S_{OUT}}{2y}\Big(1 \pm tan(\theta'(t)) tan\big(w_c t + \phi(t)\big)\Big). \tag{A.4}$$

Using A.3 to substitute the expression for S_{OUT} in A.4, we get

$$S_{PA,1/2}(t) = \frac{\alpha_o G cos\gamma}{1 + 2y^2 cos^2\gamma} cos\big(w_c t + \phi(t)\big) cos\big(\theta(t) - \gamma\big)\Big(1 \pm tan(\theta'(t)) tan(w_c t + \phi(t))\Big),$$

and replacing $tan(\theta'(t))$ with the equivalent expression from [23],

$$S_{PA,1/2}(t) = \alpha_o K G\Big[cos\big(w_c t + \phi(t)\big) cos\big(\theta(t) - \gamma\big) \pm sin(w_c t + \phi(t))\Big(\frac{sin(\theta(t) - \gamma) + 2y^2 sin\big(\theta(t)\big) cos(\gamma)}{cos(\theta(t) - \gamma)}\Big)\Big], \tag{A.5}$$

here, K is a constant for a given Chireix combiner configuration

$$K = \frac{cos\gamma}{1 + 2y^2 cos^2\gamma}.$$

The above expressions (A.5) for PA output signals are simplified to get

$$\begin{aligned} S_{PA,1}(t) &= \alpha_o G K\Big(cos\big(w_c t + \phi(t) - (\theta(t) - \gamma)\big) + y^2 cos(\gamma)\big[cos\big(w_c t + \phi(t) - \theta(t)\big) \\ &\qquad - cos\big(w_c t + \phi(t) + \theta(t)\big)\big]\Big) \\ S_{PA,2}(t) &= \alpha_o G K\Big(cos\big(w_c t + \phi(t) + (\theta(t) - \gamma)\big) + y^2 cos(\gamma)\big[cos\big(w_c t + \phi(t) + \theta(t)\big) \\ &\qquad - cos\big(w_c t + \phi(t) - \theta(t)\big)\big]\Big) \end{aligned} . \tag{A.6}$$

The above expressions articulate the transformation of PA output signal, caused by the signal reflections. These reflection effects create amplitude and phase distortion in the outphasing transmitters.

BIBLIOGRAPHY

[1] M. El-Asmar, A. Birafane, and A. B. Kouki, "Impact of PA Mismatching in Chireix-Outphasing System without Stubs," *Signals, Systems and Electronics, 2007. ISSSE '07. International Symposium on*, pp. 201–204, 7 2007.

[2] A. Birafane, M. El-Asmar, A. B. Kouki, M. Helaoui, and F. M. Ghannouchi, "Analyzing LINC Systems," in *Microwave Magazine, IEEE*, vol. 11, no. 5, 2010, pp. 59–71.

[3] B. Razavi, *RF Microelectronics (Prentice Hall Communications Engineering and Emerging Technologies Series)*, 2nd ed. Upper Saddle River, NJ, USA: Prentice Hall Press, 2011.

[4] M. E. Heidari, "An All-digital Out-phasing Transmitter for Software-defined Radio," Ph.D. dissertation, University of California at Los Angeles, 2008.

[5] P. A. Godoy, "Techniques for High-Efficiency Outphasing Power Amplifiers," Ph.D. dissertation, 2011.

[6] P. Landin, "Digital Baseband Modeling and Correction of Radio Frequency Power Amplifiers," Ph.D. dissertation, 2012.

[7] K.-L. Du and M. Swamy, *Wireless Communication Systems From RF Subsystems to 4G Enabling Technologies*. Cambridge University Press, 2010.

[8] M. Ghogho, P. Ciblat, and A. Swami, *Academic Press Library in Signal Processing: Volume 2 - Communications and Radar Signal Processing*, ser. Academic Press Library in Signal Processing. Elsevier, 2014, vol. 2.

[9] A. Mohammadi and F. M. Ghannouchi, *RF Transceiver Design for MIMO Wireless Communications*, ser. Lecture Notes in Electrical Engineering. Berlin, Heidelberg: Springer Berlin Heidelberg, 2012, vol. 145.

[10] K. C. Tsai, "CMOS Power Amplifiers for Wireless Communications," Ph.D. dissertation, Ph D Thesis, University of California at Berkeley, Electrical Engineering and Computer Sciences, 2007.

[11] B. Berglund, J. Johansson, and T. Lejon, "High efficiency power amplifiers," Ph.D. dissertation, Ericsson Reiew No. 3, 2006.

[12] F. Raab, P. Asbeck, S. Cripps, P. Kenington, Z. Popovic, N. Pothecary, J. Sevic, and N. Sokal, "Power amplifiers and transmitters for RF and microwave," *IEEE Transactions on Microwave Theory and Techniques*, vol. 50, no. 3, pp. 814–826, 3 2002.

[13] J. Yao and S. I. Long, "Power amplifier selection for LINC applications," *IEEE Transactions on Circuits and Systems II: Express Briefs*, vol. 53, no. 8, pp. 763–767, 2006.

[14] D. Kimball, J. Popp, A. Yang, D. Lie, P. Asbeck, and L. Larson, "Wideband envelope elimination and restoration power amplifier with high efficiency wideband envelope amplifier for WLAN 802.11g applications," in *IEEE MTT-S International Microwave Symposium Digest, 2005.* IEEE, 2005, pp. 645–648.

[15] P. Reynaert and M. Steyaert, "A 1.75-GHz polar modulated CMOS RF power amplifier for GSM-EDGE," *IEEE Journal of Solid-State Circuits*, vol. 40, no. 12, pp. 2598–2608, 12 2005.

[16] J. Walling, H. Lakdawala, Y. Palaskas, A. Ravi, O. Degani, K. Soumyanath, and D. Allstot, "A 28.6dBm 65nm Class-E PA with Envelope Restoration by Pulse-Width and Pulse-Position Modulation," in *2008 IEEE International Solid-State Circuits Conference - Digest of Technical Papers.* PWM_2: IEEE, 2 2008, pp. 566–636.

[17] J. S. Walling, H. Lakdawala, Y. Palaskas, A. Ravi, O. Degani, K. Soumyanath, and D. J. Allstot, "A Class-E PA With Pulse-Width and Pulse-Position Modulation in 65 nm CMOS," *IEEE Journal of Solid-State Circuits*, vol. 44, no. 6, pp. 1668–1678, 6 2009.

[18] H. Chireix, "High Power Outphasing Modulation," *Proceedings of the IRE*, vol. 23, no. 11, pp. 1370–1392, 11 1935.

[19] F. Raab, "Efficiency of Outphasing RF Power-Amplifier Systems," *IEEE Transactions on Communications*, vol. 33, no. 10, pp. 1094–1099, 10 1985.

[20] A. Ravi, P. Madoglio, H. Xu, K. Chandrashekar, M. Verhelst, S. Pellerano, L. Cuellar, M. Aguirre-Hernandez, M. Sajadieh, J. E. Zarate-Roldan, O. Bochobza-Degani, H. Lakdawala, and Y. Palaskas, "A 2.4-GHz 20–40-MHz Channel WLAN Digital Outphasing Transmitter Utilizing a Delay-Based Wideband Phase Modulator in 32-nm CMOS," *IEEE Journal of Solid-State Circuits*, vol. 47, no. 12, pp. 3184–3196, 12 2012.

[21] P. A. Godoy, S. Chung, T. W. Barton, D. J. Perreault, and J. L. Dawson, "A 2.4-GHz, 27-dBm asymmetric multilevel outphasing power amplifier in 65-nm CMOS," *IEEE Journal of Solid-State Circuits*, vol. 47, no. 10, pp. 2372–2384, 10 2012.

[22] H. Xu, Y. Palaskas, A. Ravi, M. Sajadieh, M. A. El-Tanani, and K. Soumyanath, "A Flip-Chip-Packaged 25.3 dBm Class-D Outphasing Power Amplifier in 32 nm CMOS for WLAN Application," in *Solid-State Circuits, IEEE Journal of*, vol. 46, no. 7, 2011, pp. 1596–1605.

[23] M. El-Asmar, A. Birafane, M. Helaoui, A. B. Kouki, and F. M. Ghannouchi, "Analytical Design Methodology of Outphasing Amplification Systems Using a New Simplified Chireix Combiner Model," *IEEE Transactions on Microwave Theory and Techniques*, vol. 60, no. 6, pp. 1886–1895, 6 2012.

[24] J. Hur, "A Highly Linear and Efficient Out-Phasing Transmitter for Multi-Band, Multi-Mode Applications," Ph.D. dissertation, Ph D Thesis, Georgia Institute of Technology, School of Electrical and Computer Engineering, 2010.

[25] A. Diet, C. Berland, M. Villegas, and G. Baudoin, "EER architecture specifications for OFDM transmitter using a class E amplifier," *IEEE Microwave and Wireless Components Letters*, vol. 14, no. 8, pp. 389–391, 2004.

[26] X. Zhang, L. E. Larson, and P. Asbeck, *Design of Linear RF Outphasing Power Amplifiers*. Artech House, 2003.

[27] 3GPP, "LTE; Evolved Universal Terrestrial Radio Access (E-UTRA); Base Station (BS) radio transmission and reception (ETSI TS 136 104 v9.4.0)," 3rd Generation Partnership Project (3GPP), Tech. Rep., 2010.

[28] A. F. Aref, T. M. Hone, and R. Negra, "A Study of the Impact of Delay Mismatch on Linearity of Outphasing Transmitters," *IEEE Transactions on Circuits and Systems I: Regular Papers*, vol. 62, no. 1, pp. 254–262, 1 2015.

[29] E. Nash, "An-1039 application note: Correctin Imperfections in IQ Modulators to Improve RF Signal Fidelity," pp. 1–8.

[30] L. Sundstrom, "Spectral sensitivity of LINC transmitters to quadrature modulator misalignments," *IEEE Transactions on Vehicular Technology*, vol. 49, no. 4, pp. 1474–1487, 7 2000.

[31] M. Faulkner and T. Mattson, "Spectral Sensitivity of Power Amplifiers to Quadrature Modulator Misalignment," *IEEE Transactions on Vehicular Technology*, vol. 41, no. 4, pp. 516–525, 1992.

[32] J. Vuolevi and T. Rahkonen, *Distortion in RF Power Amplifiers*. Artech House, 2003.

[33] W. Gerhard and R. Knöchel, "Prediction of bandwidth requirements for a digitally based WCDMA phase modulated outphasing transmitter," *Technology*, 2005.

[34] B. Razavi, *Principles of Data Conversion System Design.* Wiley-IEEE Press, 1994.

[35] C. Conradi, R. Johnston, and J. McRory, "Evaluation of a lossless combiner in a LINC transmitter," *Engineering Solutions for the Next Millennium. 1999 IEEE Canadian Conference on Electrical and Computer Engineering (Cat. No.99TH8411)*, vol. 1, pp. 105–110, 1999.

[36] D. M. Pozar, *Microwave Engineering*, 4th ed. Wiley, 2012.

[37] A. Birafane and A. B. Kouki, "On the linearity and efficiency of outphasing microwave amplifiers," *IEEE Transactions on Microwave Theory and Techniques*, vol. 52, no. 7, pp. 1702–1708, 2004.

[38] "MATLAB, version 8.5 (R2015a)," Natick, Massachusetts, 2015.

[39] A. Ghorbani and M. Sheikhan, "The effect of solid state power amplifiers (SSPAs) nonlinearities on MPSK and M-QAM signal transmission," pp. 193–197, 1991.

[40] R. C. Li, *RF Circuit Design.* Wiley, 2012.

[41] J. D. Taylor, *Introduction to Ultra-Wideband Radar Systems.* Taylor & Francis, 1994.

[42] J. Lemberg, M. Kosunen, E. Roverato, M. Martelius, K. Stadius, L. Anttila, M. Valkama, and J. Ryynanen, "Digital Interpolating Phase Modulator for Wideband Outphasing Transmitters," *IEEE Transactions on Circuits and Systems I: Regular Papers*, pp. 1–11, 2016.

[43] A. Birafane and A. B. Kouki, "Phase-only predistortion for LINC amplifiers with Chireix-outphasing combiners," pp. 2240–2250, 2005.

[44] A. Huttunen and R. Kaunisto, "A 20-W Chireix Outphasing Transmitter for WCDMA Base Stations," pp. 2709–2718, 2007.